Letter to the Editor

Bremen, 22.07.2019

Dear Michel Van Roozendael,

we would like to take the opportunity to thank you for editing our manuscript on MAX-DOAS measurements of ship emissions. As suggested by both referees, we updated and expanded the described method by incorporating ship plume modeling using a simple Gaussian plume model and combining it with the plume forward trajectories, allowing to derive in-plume NO2 VMRs from the MAX-DOAS measurements without the need of accompanying airborne measurements. The AirMAP measurements are now only used for validation of both the plume modeling and the MAX-DOAS results. To reflect this, we changed the title from "Studies of the horizontal inhomogeneities in NO_2 concentrations above a shipping lane using ground-based MAX-DOAS and airborne imaging DOAS measurements" to the new title "Studies of the horizontal inhomogeneities in NO_2 concentrations above a shipping lane using ground-based MAX-DOAS measurements *and validation with* airborne imaging DOAS measurements".
We individually answered point-by-point to all comments and questions of Referee #1 and Referee #2. We revised the original manuscript according to their suggestions and provided additional information the referees asked for.

Below, you find again the answers to the referees that we also uploaded to the AMT web page. We also provide here a version of the revised manuscript in which changes in comparison to the initial version are marked color-coded. In addition to that, a version of the manuscript in the Copernicus two-column style (using the Copernicus Latex-Template) is attached.
We hope that with the submission of the author's comments and the revision of the manuscript, our article can be accepted for publication in AMT.

Yours sincerely,

André Seyler

List of Attachments

- Author comments to Referee #1
- Author comments to Referee #2
- Revised manuscript with color-coded changes

Atmos. Meas. Tech. Discuss., doi:10.5194/amt-2018-348-RC1, 2018

Atmospheric Measurement Techniques Discussions

Interactive comment on "Studies of the horizontal inhomogeneities in NO_2 concentrations above a shipping lane using ground-based MAX-DOAS and airborne imaging DOAS measurements" *by* André Seyler et al.

Anonymous Referee #1

Received and published: 12 December 2018

GENERAL COMMENTS

The manuscript "Studies of the horizontal inhomogeneities in NO2 concentrations above a shipping lane using ground-based MAX-DOAS and airborne imaging DOAS measurements" presents nicely and picturesque the onion peeling approach applied to measurements in the German bight, demonstrated on individual measurements. In the second part of the manuscript, the authors compare 2 specific measurement instances to airborne imaging DOAS measurements taken during the NOSE campaign. These two instances show well the validity of the onion peeling approach, qualitatively and quantitatively.
While this second part, the comparison with imaging doas, makes also quantitative estimates, the first part, showing two times example measurements within approximately 12 minutes in 5 different azimuth directions, stays very qualitative. It neither includes an estimation of errors by e.g. the negligence of the correction factor in the O4 scaling approach for the effective light path estimation, nor does it include an attempt of making use of some ancillary information about the plume using e.g. the STEM model (Jalkanen et al. 2009 acp 9209-9223 , 2012 acp 2641-2659) and some diffusion model to estimate plume width/ height.
The authors argue that the presented method is suited to measure concentrations when wind conditions are unsuitable for surface measurements which do not measure any enhanced concentration if the wind blows the plume away from the measurement station. However, they themselves mention that the measured concentration with the onion peeling approach is not representative of the in-plume concentration. The authors lack to investigate possibilities how to extract useful information using other available information (using more info from the AIS data in combination with the STEM model and better modelling of the plumes). No attempt was made to connect the measured concentration to the in-plume concentration in the first part of the paper. Even if this is not carried out, I strongly recommend the authors to think about ways how this could be done and at least describe what could be done. Without it, this method seems rather incomplete and its usefulness quite limited.

However, the paper is very well presented and shows that if complementary measurements are available, useful estimates about plume concentrations of individual plumes can be calculated and hence should be published! It remains nevertheless unclear what the main purpose of the measurements is if no connection can be made to the in-plume concentration. This could certainly be clarified better both in the introduction and in the conclusions. I recommend to either include attempts to extract more information about the actual plume concentrations by using more ancillary information in

the first part of the paper (basically describing Fig. 6, 7, 8 and 9) or skipping that part and only concentrating on the second part. In the current state, it is a long paper that, over big parts, is rather qualitative and does not give much quantitative information about plume concentrations and hence is not quite suited for measurements of ship emissions on its own.

First, we would like to thank Anonymous Referee #1 for his/her helpful comments, particularly concerning the suggestion for the inclusion of ship plume modeling.

We updated and enhanced the described method by incorporating ship plume modeling using a simple Gaussian plume model and combining it with the plume forward trajectories. The information about plume width and height retrieved from the model is then used to derive in-plume volume mixing ratios of NO_2 from the MAX-DOAS measurements without the need for the airborne imaging DOAS measurements. In the new version, the AirMAP measurements are now only used for validation. As a consequence, the structure and aim of the paper was adapted. Section 5 was completely rewritten (now: Section 4.4) and contains two parts: The first part contains a technical demonstration of the method to derive in-plume NO_2 VMRs from MAX-DOAS measurements for ships passing the instrument in a distance of several km. We decided to demonstrate the method on the measurements during the NOSE campaign shown in Fig. 10 (new: Fig. 8), as AirMAP measurements for validation are available for this day.

In the second part of Section 4.4, the AirMAP measurements are used for validating both the plume modeling and the MAX-DOAS results. The modeled plume location and shape (including the plume width) is compared to the AirMAP measurements. The vertical plume extent from the model is compared to the estimation from the MAX-DOAS vertical scan, which was already included in the previous version. As before, the approximate plume position retrieved with the onion peeling MAX-DOAS approach is compared to the AirMAP measurements. The in-plume NO_2 VMR derived from the MAX-DOAS measurements is now compared to the in-plume VMR computed for the AirMAP measurements with help of the modeled plume height.

We kept the general structure, as we think the order of the results facilitates comprehension by enabling the readers to go step-by-step from the more basic time-series plots to the complex map figures which contain a lot of information. Starting with the time-series showing the relation between DSCDs and path-averaged VMRs, then taking the step from the time-series to the map figures with colored lines representing the VMRs and path lengths (for northerly and southerly wind directions) and finally the step to the figures additionally including the AirMAP measurements showing two completely different quantities: for AirMAP vertical columns of NO_2, for MAX-DOAS path-averaged NO_2 VMRs.

We think that the inclusion of plume modeling allowing derivation of in-plume NO_2 VMRs from MAX-DOAS measurements without the need of airborne measurements makes the paper scientifically more relevant and the described method much more quantitative and the main purpose of the measurements becomes clearer.

Below, we reply point-by-point to the specific comments. As far as possible, we have considered the suggestions in the revised manuscript.

SPECIFIC COMMENTS

(a) The authors only mention the restrictions on sulphur emission by the MARPOL convention. However, this manuscript is about NO2, so it should probably also give the info on this. Something like... EU adaption of this in form of directive 2012/33/EU NOx emissions depends on the rated rotational speed of the engine crankshaft, implementation in 3 tiers, last one not yet implemented, shifted to ~2021

Thank you very much, we must have overlooked this. Of course, the manuscript should mention the MARPOL NO_x emission regulations in the North and Baltic sea (N)ECA. A corresponding paragraph has been added to the text.

(b) In the last paragraph of Sect. 3.2, the authors mention the importance of NO to NO2 conversion. Maybe the authors can give some estimates on time- (and spatial) scales for the increase (probably depending on some "standard"(?) background O3 concentration).

Some unpublished measurements performed at another site under roughly similar conditions indicate that already after a few minutes, the fraction of NO_2 in the overall NO_x is quite high. After 1 minute, the NO content on the overall NO_x is below 60% for most ships (but up to 96 % for some), after 3 minutes it drops to values below 40% for most ships (but up to 70-80% for some). After 5 minutes it is below 25% for most ships and after 8-10 minutes it is below 20-30% for all ships. Of course, this depends on the ambient ozone concentration.

Middleton et al. (2007)[1] modeled the NO to NO_2 conversion in plumes at short ranges, depending on the O_3 concentration:

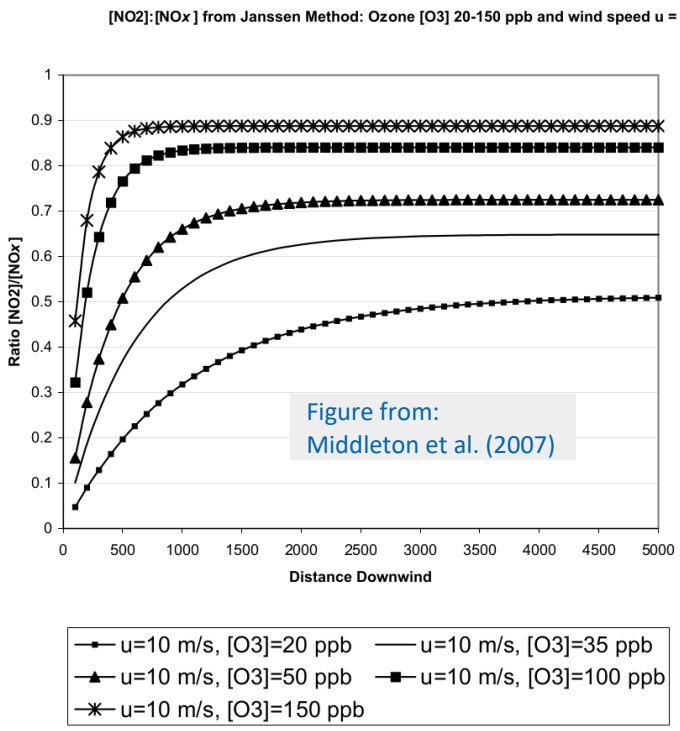

Figure 1
Plot of results for the yield or ratio $[NO_2]$:$[NO_x]$ using the Janssen (Janssen 1986, Janssen *et al*. 1988) method of near-source diffusion-limited O_3, which soon becomes asymptotic to the photostationary state further from the source, after approximately 200 seconds of travel time (2 km downwind here). The effect of changes in O_3 concentration is shown. The wind speed alters the choice of curve according to travel time (distance/speed). (In these curves distance is plotted on the x-axis; empirical curves later in this report show NO_x on the x-axis.)

The figure shows that both the steady state value of the NO_2 to NO_x ratio as well the time until the steady state is reached depend on the O_3 concentration.

At our Neuwerk station, typical background O_3 volume mixing ratios in summer are in the range of 30 to 40 ppb, but can go up to 60-70 ppb or down to 20 ppb as well. Taking a closer look at the curves for 35 ppb and 50 ppb ambient O_3 in the figure, it can be seen that the steady state is predicted to be reached already after 3 to 4 minutes and in the steady state the fraction of NO_2 on the overall NO_x is 65-70%. This fits quite well to our measurements mentioned above.

Meier (2018)[2] shows AirMAP NO_2 measurements during an overflight over a ship and its plume from the NOSE campaign on 21 August 2013. The across−plume integrated NO_2 VCD increases with flown distance from the ship overpass, stabilizing on a plateau at a distance of around 3 km. This 3 km are not the distance since emission, as the plume is moved by the wind during the time from ship overpass to this point. Taking the combination of plume forward trajectories and simple Gaussian plume model, the plume age at this point is estimated to be ~400 seconds or ~6.5 minutes, in which the emitted air parcels traveled a distance of ~1.5 km. This is in the same order of magnitude than the measurements and model results discussed above.

[1] Middleton, D. R., Luhana, L. and Sokhi, R. S.: Review of methods for NO to NO2 conversion in plumes at short ranges, Environment Agency, Bristol., 2007.

[2] Meier, A. C.: Measurements of Horizontal Trace Gas Distributions Using Airborne Imaging Differential Optical Absorption Spectroscopy, phd thesis, University of Bremen, Bremen., 2018.

To conclude, after a few minutes, at the latest after 10 minutes, the NO to NO_2 conversion reaches its steady state, depending on the ambient ozone concentration. As the plumes considered in the manuscript are usually older than 10 minutes, NO to NO_2 titration should not have a strong influence on the presented results.

A summary of this information was included into the last paragraph of Section 3.2.

Also, the authors mention in Sect. 3.3 that plume broadening and dilution over time is neglected. Maybe an order of magnitude estimation should be included and it should be outlined how this information can be used to extract more useful information from the measurements. Which of the two effects dominates for which time-scales? Maybe a reference to some dispersion models that include chemistry?

As outlined above, we have added plume modelling to the manuscript which addresses this point at least partly.

(c) In Sect. 3.3 it is stated that the initialization period is 90 minutes before the measurements. The big plume (roughly N-S direction) present in all panels in Figure 8 (and 9), originates, according to the authors (Sect. 4.3 3rd paragraph) from two coal-fired power plants in Wilhelmshaven, 50 km away. The authors estimate the plume age to be 110 minutes. However, this suggests that the initialization period needed to be larger than 90 minutes, otherwise the plume would not have had the time to travel that far. I think this should be clarified.

After double-checking the numbers, it turned out that 90 minutes is in fact not correct. The applied initialization time for both case studies is 180 minutes (3 hours). This was corrected in the manuscript.

(d) Regarding the plume trajectories, maybe the "apparent wind" approach as illustrated e.g. in Berg et al (2012, amt 1085-1098) should be referenced.

Done.

(e) It is mentioned that there are two stations measuring wind conditions, one on Neuwerk, one on Scharhörn. However, it is not clear whether the wind used for the calculation of the plume trajectories in e.g. Fig. 6 or Fig.8 is a simple average of the two, or if it depends on the position of the plume at every given moment which wind (some sort of spatial interpolation) is applied, or if only one is used. Please clarify.

Depending on data availability and data quality, either wind data from the Scharhörn or Neuwerk weather station was used. Added a hint to the source of the weather data at the respective places in the text.

(f) Regarding the author's comment to Fig. 6 panel 1 why the plume of the small ship is not seen: Maybe the authors could do a quick calculation which heights are seen at the expected distance of the plume (about from about 20–40 m ?). What do the authors find more likely? Maybe using the STEAM model for that particular ship, together with estimates for the dilution due to diffusion and NO to NO2 conversion the authors could approximate in plume concentration and exclude or not exclude their first alternative.

The plume model gives the following results for this situation:

- plume age: 700-800 seconds,
- plume width: 1200-1300m,
- plume height: ~400m (reaching down to the ground) for a stack height of ~25 meters

It is therefore not likely, that the MAX-DOAS did not measure through the plume. NO to NO_2 titration (see above) also tells us that NO_x is (very) roughly 80% NO_2 at this plume age. So the second alternative is also not likely. It is more likely, that the plume from this relatively "small" ship, which is quite strongly dispersed already, is also strongly diluted. If the amount of NO_x emitted by this ship is relatively small, this might not be visible in the MAX-DOAS measurements.

To take this into account, the sentence was rewritten and now reads: “The fact that the plume from the smaller ship shows up only slightly in the measurements might be due to low emissions from this comparatively small ship and the dilution of the already strongly dispersed plume, as the plume model predicts a vertical extent of the plume of ~400 m and a plume width of 1200-1300 m at a plume age of 700-800 seconds.”

(g) Can the authors comment on the effect on the MAXDOAS results when the plume is over the instrument, as also indicated by high in-situ measurements? Does this lead to cancelling effects or is the vertical extend of the plume negligible comparable to the horizontal?

This can be investigated by looking at the zenith sky measurements. For this, a different type of DOAS fit had to be done, using a noon reference[3] instead of the sequential reference[4] spectrum used in this study. The results can be seen in the following figure, showing the UV NO_2 DSCD for both off-axis measurements (0.5°, 1.5°, 2.5°, 3.5°, 4.5° and 30° elevation) in the 335° azimuth direction and zenith sky measurements (90° elevation) for the same day as in Fig. 6 (new: Fig. 4).

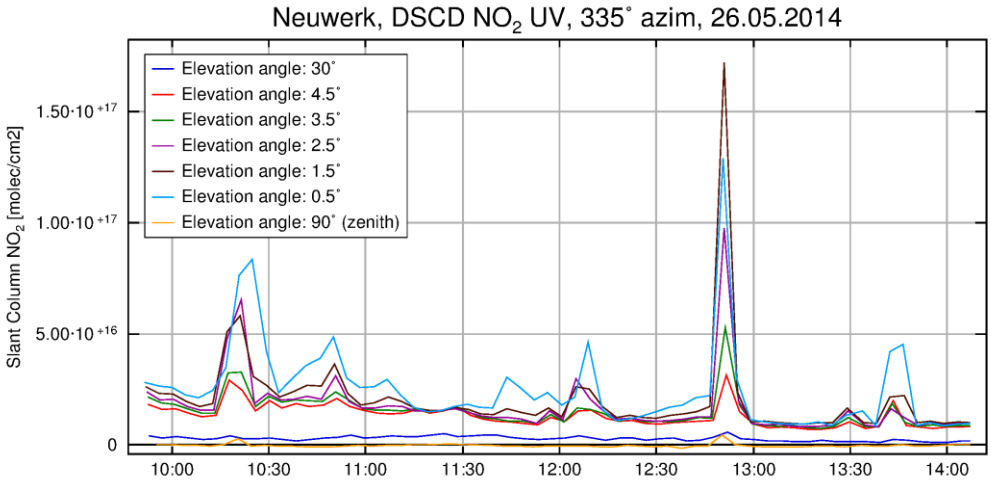

The zenith sky measurements (orange line, close to zero) indeed show enhanced values on this day, around 10:20 UTC and also around 12:50 UTC, at the very time of the respective situation in Fig. 6 (new: Fig. 4) when the plumes are reaching the radar tower/are over the instrument and in-situ values are high. At 12:50-12:53 UTC, a maximum NO_2 DSCD of 4×10^{15} molecules/cm^2 is measured. Nevertheless, compared to the measurements in the 0.5° elevation used for the onion peeling reaching up to 1.3×10^{17} molecules/cm^2 and in 1.5° elevation reaching even up to 1.7×10^{17} molecules/cm^2, this number is small. While the vertical extent of the plume is certainly not negligible (the model says 400-450 m), it seems to have only a small influence on the zenith sky measurements because of the short vertical light path. This NO_2 enhancement in the zenith sky measurements definitely causes a canceling effect when using the sequential reference, but the overall impact seems to be negligible small (2 to 4 %). We added the following sentences to the text:

“A small NO_2 enhancement of 4×10^{15} molec/cm^{-2} is seen in the zenith sky measurements around 12:50 UTC, which is gone at 12:55 UTC, indicating that at least part of the plume was located above the MAX-DOAS instrument. As the zenith sky measurements are used as a sequential reference for the off-axis measurements, this causes a small canceling effect when using the sequential reference. As off-axis DSCDs are on the order of 1×10^{17} molec/cm^{-2} reaching up to 1.4×10^{17} molec/cm^{-2} as can be seen from Fig. 3, the overall impact on the path averaged VMRs is very small, on the order of 2 to 4 %.”

[3] one zenith spectrum at noon is taken as the reference spectrum for this day

[4] for each spectrum a close-in-time interpolated zenith spectrum is taken as a reference

(h) Fig6, panel 10: The plume from the big ship cannot have yet reached the VIS-only region (Delta L). However, compared to the measurement 4 minutes before, the VMR seems to have increased by around 1.5 ppb. Any suggestion why?

There is definitely an increase in the NO_2 DSCDs measured in the visible from 0.9 ppb to 1.6 ppb. The following figure shows both the off-axis measurements (0.5° and 2.5° elevation) for this viewing direction (310° azimuth) and the zenith sky measurements in the visible:

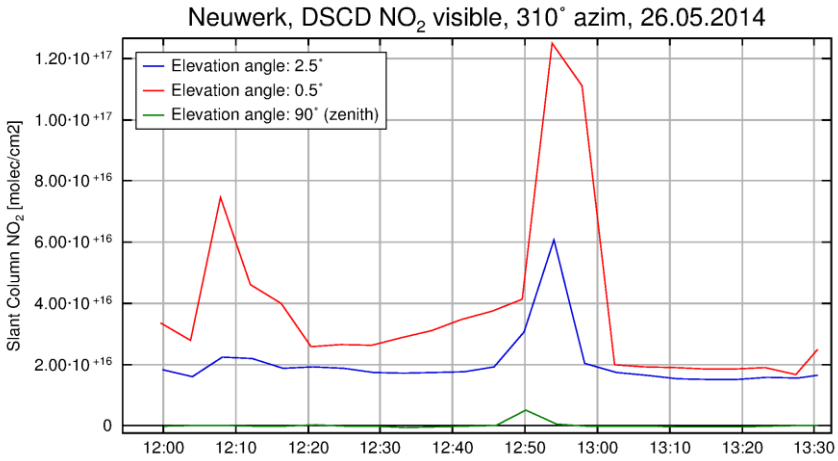

Possible reasons could be emissions from another ship, the AIS signal of which was not received or emissions from a land-based source somewhere at the west-coast of Schleswig-Holstein, which is quite unlikely. More likely, however, is an uncertainty (overestimation) in the path length estimation due to negligence of the correction factor (see next question below), meaning that this increase is already coming from the ship crossing the line-of-sight in Panel 15. As can be seen from the measurements in the figure shown above, the NO_2 values drop quickly to ambient background values 4 minutes after Panel 15 when ship and plume have fully crossed the LOS and are now westward of it.

(i) Similarly, panel 15 seem to indicate a larger intersect of the plume with the viewingdirection for the UV region than for the VIS-only region. Still it looks like (as mentioned below, maybe not the best choice of colour map) the VIS-only region has a much higher average VMR. Probably this is due to the effect of overestimated length (due to negligence of correction factor as mentioned by the authors) and hence more of the intersection is in the UV-only path?

In fact this might be an example showing the uncertainty (overestimation) in the path length estimation due to negligence of the correction factor. The following paragraph was added to the manuscript:

"In Panel 15 the larger ship has moved further away from the instrument, leading for the first time in this sequence to a higher concentration on ΔL, far away from the instrument, than close by. Comparing the locations of the MAX-DOAS paths with the ship position and modeled plume in detail, however, indicates a much larger intersect of the plume with the UV path than with ΔL. This might be an example showing the uncertainty (overestimation) in the path length estimation due to negligence of the correction factor as discussed in Section 3.1."

(j) The first two (not numbered) equations seem to indicate that the air density in fact cancels out in the authors approach to estimate the VMR since only surface values for concentrations?

The air density does not cancel out, because the number density of O_4 contains the square of the number density of air, as $n_{O4} = (0.21 \cdot n_{O2})^2$. The first equation is therefore:

$$L = \frac{\mathrm{SCD}_{\mathrm{O_4,horiz}} - \mathrm{SCD}_{\mathrm{O_4,zenith}}}{n_{\mathrm{O_4}}} = \frac{\mathrm{DSCD}_{\mathrm{O_4}}}{n_{\mathrm{O_4}}} = \frac{\mathrm{DSCD}_{\mathrm{O_4}}}{(n_{\mathrm{O_2}})^2} = \frac{\mathrm{DSCD}_{\mathrm{O_4}}}{(0.20942 \cdot n_{\mathrm{air}})^2}$$

Inserting the first equation for the path length into the second equation yields:

$$\mathrm{VMR}_{\mathrm{NO_2}} = \frac{\mathrm{SCD}_{\mathrm{NO_2,horiz}} - \mathrm{SCD}_{\mathrm{NO_2,zenith}}}{L \cdot n_{\mathrm{air}}} = \frac{\mathrm{DSCD}_{\mathrm{NO_2}}}{L \cdot n_{\mathrm{air}}}$$
$$= \frac{\mathrm{DSCD}_{\mathrm{NO_2}} \cdot (0.20942 \cdot n_{\mathrm{air}})^2}{\mathrm{DSCD}_{\mathrm{O_4}} \cdot n_{\mathrm{air}}} = \frac{\mathrm{DSCD}_{\mathrm{NO_2}} \cdot 0.20942^2 \cdot n_{\mathrm{air}}}{\mathrm{DSCD}_{\mathrm{O_4}}}$$

Note that the units, at a first glance maybe counter-intuitive, do fit together here: [$DSCD_{NO2}$] = molecules/cm^2, [n_{air}] = molecules/cm^3, [$DSCD_{O4}$] = $molecules^2/cm^5$,

fitting to the unit-less quantity VMR.

(k) The title suggests a more "equal weight" between the two methods in terms of "being presented". However, the imaging approach seems to be merely used for validation and is not presented as such, since this is done in a different publication. Maybe the title should reflect this.

The title was changed to reflect this.

(l) The authors conclude in their last sentence of the manuscript that this approach canbe successfully applied to ship emission measurements. Nowhere in the paper is an estimation of the ship emission presented. I advice the authors to delete or reformulate this sentence.

The sentence was reformulated and now reads: “To conclude, the presented measurements provide a real world demonstration that the onion peeling approach works for MAX-DOAS measurements and can successfully be applied to investigate air pollution by ships and to derive in-plume NO_2 volume mixing ratios for ships passing the instrument in a distance of several km.”

TECHNICAL CORRECTIONS AND SUGGESTIONS

(a) page 2, line 31: ... is of (not on) the order of….

Done.

(b) page 5/6: 2 equations on these sides are not labelled. I think all equations shouldbe labelled.

Corrected.

(c) page 8, last sentence of penultimate paragraph: This is a really confusing sentence. I would probably reformulate to something like: "The movement of the ship together with the measured wind results in an apparent wind direction very different from the measured wind direction. Therefore, a measurement along the measured wind direction does not in genereal correspond to measurements along the plume".

Reformulated the sentence to: “But as the movement of the ship together with the measured wind can result in an apparent wind direction very different from the measured wind direction a measurement along the measured wind direction does not in general correspond to measurements along the plume. “

(d) Fig. 3,4 and 5: For easier reference, it might be a good idea to bundle those intoone figure with 3 vertically aligned panels.

Done. The three figures are now bundled into one figure with three panels.

(e) Fig 6 and 8: maybe a length scale would be nice to include.

Good idea. A length scale was included into the figures. To not overly clutter the small maps, it is shown only in the first panel of each figure.

Also, I suggest to label the viewing directions on the right-hand side on each row.

A very good idea! As suggested, I included labels for the azimuthal viewing directions on the RHS.

I am not sure if a jet-like colour scale is the best choice. The gnuplot type one used in Fig. 1 or viridis or any other colour scale that is monotone in lightness (The first and the last comment also hold for Fig. 7 and 9) would be better. However, maybe that is just something the authors can keep in mind for the next publication.

As you have already noticed, "Plasma", one of the new perceptually uniform sequential colormaps introduced with *Python* package *Matplotlib* version 2, was used for the ship traffic density map in Fig. 1. For the onion-peeling maps (e.g. former Fig. 6-9, new: Fig. 4-7), the usage of the colormap "Viridis" was tried before but turned out to be problematic, because in the printed version of the figures, the dynamic range of the colormap was too small. Here as an example the scanned version of a print out of Figure 9 (new: Fig. 7):

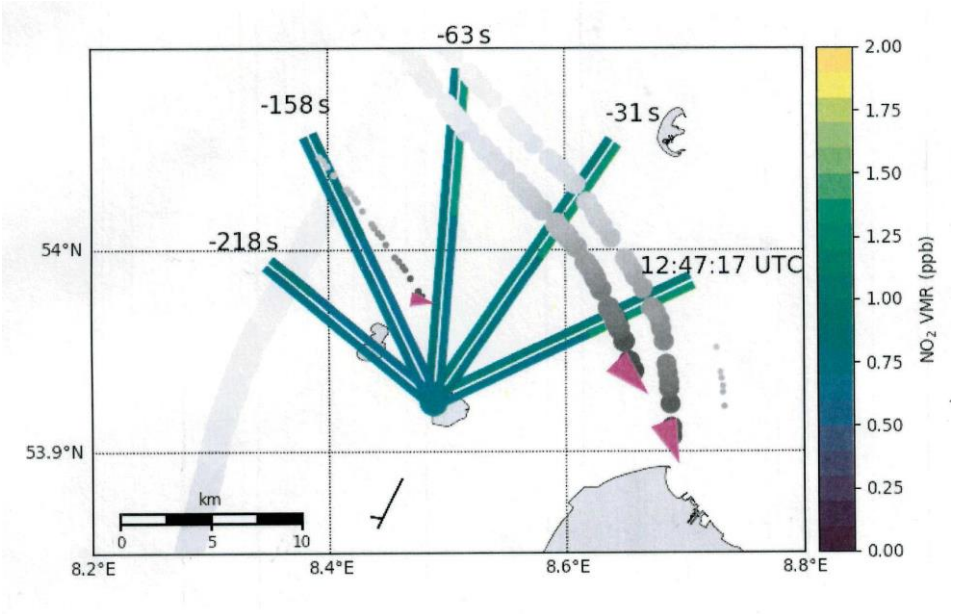

In the printed version, NO_2 VMRs between ~0.6 and ~1.4 ppb have virtually the same color shade and are undistinguishable. An adjustment of the colorscale in this figure only using a smaller range of values makes the colorscale inconsistent with Fig. 8 (new: Fig. 6), where nearly the full range is needed. So we decided to use the colormap "jet", even though we are aware of the disadvantages of jet-like colormaps and the accompanying problems and try to avoid it as much as possible. However, in the last figures where MAX-DOAS and AirMAP measurements are shown in the same plot, we changed the AirMAP color-scale to viridis to better distinguish visually between the two.

(f) page 13, line 2: "lightboth"??

Corrected.

(g) page 14, Sect. 4.3, second paragraph: Figure 8... (not Figure 6)

Corrected.

(h) Figures 1,6,7,8, and 9: Can the authors quickly state why Nigelhörn and Scharhörn got merged into one island in their map?

This is an interesting point. The coastlines included in the maps are shapefiles produced from OpenStreetMap (OSM) coastline data. The maps were created with the python package "Basemap" which incorporates another coastline data set, the GSHHG (Global Self-consistent, Hierarchical, High-resolution Geography Database), formerly known as GSHHS (Global Self-consistent, Hierarchical, High-resolution Shorelines). Coastlines can also be extracted from the GADM Database of Global Administrative Areas. The following three maps show the outlines of the islands Neuwerk, Scharhörn and Nigehörn in the different data sets:

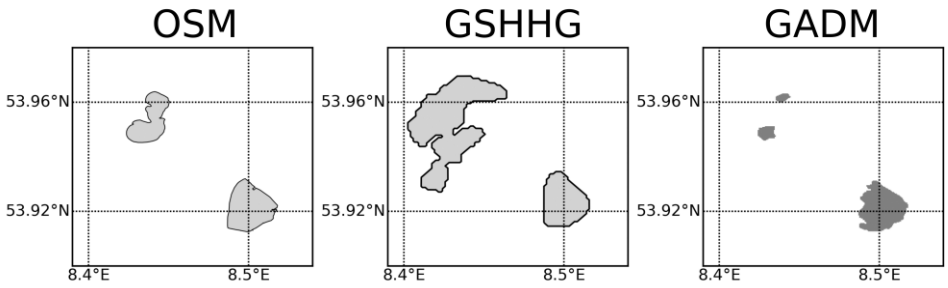

In the OpenStreetMap data, the two islands Nigehörn and Scharhörn are connected (I also wondered about that). In the GSHHG data set (this is already the highest resolution), they do look very strange. In the GADM data set, they are separated, but the problem with using the GADM data set is, that the western coastline of the island Neuwerk has a very strange shape, which does not reflect the reality.

So, which data set is better? Some deeper research revealed that the answer to this question is not so clear. Off course, when the artificial island Nigehörn was created in 1989 by deposition of 1.2 million cubic metres of sand on the "Scharhörnplate" sandbank, both were separate islands. But in the following decades, Nigehörn naturally grew on the wadden sea side, towards the east, from 30 ha in 1989 to about 50 ha in 2004. Both islands are growing together (coalesce) and the wadden sea ground between the islands on the Scharhörnplate is growing in height. Since a few years the islands are somehow "connected" by a growing salt marsh (salt meadow), which is largely safe from flooding during high tide. In the future, the islands will grow together.

(Sources:
https://de.wikipedia.org/wiki/Nigeh%C3%B6rn,
https://www.nationalpark-wattenmeer.de/hh/luftbildpanoramen/spots/scharhoern-ost03,
http://nationale-naturlandschaften.de/gebiete/nationalpark-hamburgisches-wattenmeer/,
all visited on 18.05.2019)

This can even be seen on satellite maps:

So the question whether the islands Nigehörn and Scharhörn should be separate on a map or not, cannot be answered so clearly. The shape of Scharhörn and Nigehörn seen in the satellite map fits nicely to the OSM coastline data and the OSM coastline has the best representation of the Neuwerk coastline, too. This is why it was chosen for the map plots.

Atmos. Meas. Tech. Discuss., doi:10.5194/amt-2018-348-RC2, 2019

Atmospheric Measurement Techniques Discussions

Interactive comment on "Studies of the horizontal inhomogeneities in NO_2 concentrations above a shipping lane using ground-based MAX-DOAS and airborne imaging DOAS measurements" *by* André Seyler et al.

Anonymous Referee #2

Received and published: 4 January 2019

This paper presents measurements of NO2 from ship emissions in the German Bight using MAX-DOAS instrument, and shows that horizontal information on the NO2 distribution can be derived using an onion peeling method with NO2 slant columns derived separately in the UV and visible, which are observing slightly different air masses. The authors show two case studies of different wind directions, and use coincident airborne remote sensing observations of plume extents to derive mixing ratios from the MAXDOAS measurements.

The paper is concisely written, well-organized and logical. The figures are very clear and easy to follow. Overall I found the paper interesting and recommend it be eventually published. I did find it somewhat lacking in a description of motivation for the work and its possible application. The method for deriving horizontal information from MAXDOAS using onion peeling was previously demonstrated for an urban area, and this paper is now applying it to ship emissions. This seems useful in theory, but it's not clear how the information would be used. Without plume extent information, the VMRs are derived over a long path in Section 4. Section 5 uses the airborne information to derive more precise VMR inside the plume, but these airborne measurements are rare and not regular. What would be the purpose of the MAX-DOAS measurements over a long time period? Would they be useful for trends, emissions estimates, monitoring etc? How can this be accomplished without plume width information, and are there other sources of this information? Can better modeling of ship plumes and NOx chemistry improve the estimates?
Also, aerosols, plume height and a few other sources of errors are quickly mentioned in Section 3.1, and clouds are quickly mentioned in Section 4.1. However, there is no thorough quantitative error assessment. I think the error sources need to be discussed and quantified in more detail. If you don't want to get into clouds, at least mention that for now you will only consider and draw conclusions about clear days.

Also, error sources for the the AirMAP measurements should be described. There is an uncertainty given, but it is not clear from where it is derived. There are many possible error sources (fitting uncertainty, surface albedo, profile shape, aerosols etc).

First, we would like to thank Anonymous Referee #1 for his/her helpful comments, particularly concerning the suggestion for the inclusion of ship plume modeling.

We updated and enhanced the described method by incorporating ship plume modeling using a simple Gaussian plume model and combining it with the plume forward trajectories. The information about plume width and height retrieved from the model is then used to derive in-plume volume mixing ratios of NO_2 from the MAX-DOAS measurements without the need for the airborne imaging DOAS measurements. In the new version, the AirMAP measurements are now only used for validation. As a consequence, the structure and aim of the paper was adapted. Section 5 was completely rewritten (now: Section 4.4) and contains two parts: The first part contains a technical demonstration of the method to derive in-plume NO_2 VMRs from MAX-DOAS measurements for ships passing the instrument in a distance of several km. We decided to demonstrate the method on the measurements during the NOSE campaign shown in Fig. 10 (new: Fig. 8), as AirMAP measurements for validation are available for this day.

In the second part of Section 4.4, the AirMAP measurements are used for validating both the plume modeling and the MAX-DOAS results. The modeled plume location and shape (including the plume width) is compared to the AirMAP measurements. The vertical plume extent from the model is compared to the estimation from the MAX-DOAS vertical scan, which was already included in the previous version. As before, the approximate plume position retrieved with the onion peeling MAX-DOAS approach is compared to the AirMAP measurements. The in-plume NO_2 VMR derived from the MAX-DOAS measurements is now compared to the in-plume VMR computed for the AirMAP measurements with help of the modeled plume height.

We kept the general structure, as we think the order of the results facilitates comprehension by enabling the readers to go step-by-step from the more basic time-series plots to the complex map figures which contain a lot of information. Starting with the time-series showing the relation between DSCDs and path-averaged VMRs, then taking the step from the time-series to the map figures with colored lines representing the VMRs and path lengths (for northerly and southerly wind directions) and finally the step to the figures additionally including the AirMAP measurements showing two completely different quantities: for AirMAP vertical columns of NO_2, for MAX-DOAS path-averaged NO_2 VMRs.

We think that the inclusion of plume modeling allowing derivation of in-plume NO_2 VMRs from MAX-DOAS measurements without the need of airborne measurements makes the paper scientifically more relevant and the described method much more quantitative and the main purpose of the measurements becomes clearer.

Adding NO_x chemistry to the plume model would certainly improve the results but would also be more challenging. As the plumes measured in the study are mostly rather old (plume age usually > 10 minutes), we expect most of the NO to be already converted to NO_2. Some unpublished measurements performed at another site under roughly similar conditions indicate that already after a few minutes, the fraction of NO_2 in the overall NO_x is quite high. After 1 minute, the NO content on the overall NO_x is below 60% for most ships (but up to 96 % for some), after 3 minutes it drops to values below 40% for most ships (but up to 70-80% for some). After 5 minutes it is below 25% for most ships and after 8-10 minutes it is below 20-30% for all ships. Of course, this depends on the ambient ozone concentration.

Middleton et al. (2007)[1] modeled the NO to NO_2 conversion in plumes at short ranges, depending on the O_3 concentration:

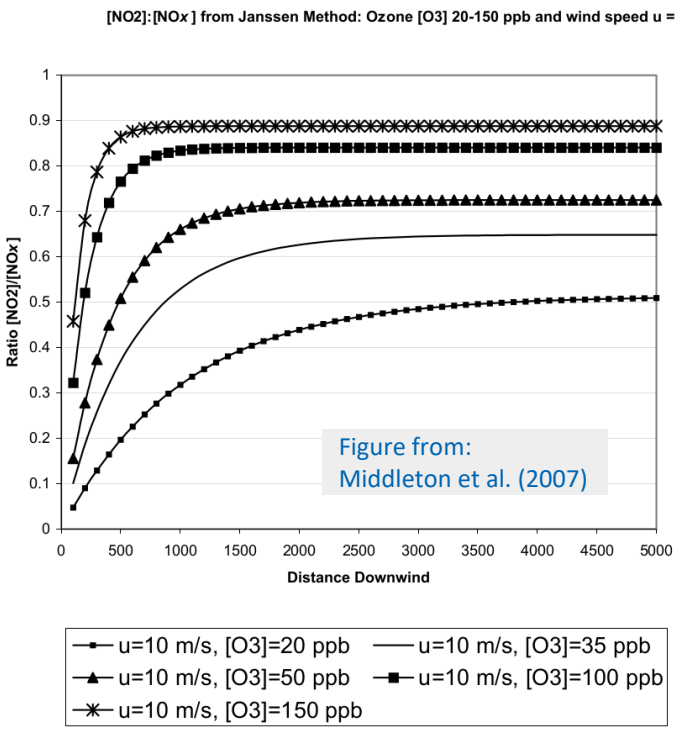

Figure 1
Plot of results for the yield or ratio $[NO_2]$:$[NO_x]$ using the Janssen (Janssen 1986, Janssen *et al*. 1988) method of near-source diffusion-limited O_3, which soon becomes asymptotic to the photostationary state further from the source, after approximately 200 seconds of travel time (2 km downwind here). The effect of changes in O_3 concentration is shown. The wind speed alters the choice of curve according to travel time (distance/speed). (In these curves distance is plotted on the x-axis; empirical curves later in this report show NO_x on the x-axis.)

The figure shows that both the steady state value of the NO_2 to NO_x ratio as well the time until the steady state is reached depend on the O_3 concentration.

At our Neuwerk station, typical background O_3 volume mixing ratios in summer are in the range of 30 to 40 ppb, but can go up to 60-70 ppb or down to 20 ppb as well. Taking a closer look at the curves for 35 ppb and 50 ppb ambient O_3 in the figure, it can be seen that the steady state is predicted to be reached already after 3 to 4 minutes and in the steady state the fraction of NO_2 on the overall NO_x is 65-70%. This fits quite well to our measurements mentioned above.

Meier (2018)[2] shows AirMAP NO_2 measurements during an overflight over a ship and its plume from the NOSE campaign on 21 August 2013. The across−plume integrated NO_2 VCD increases with flown distance from the ship overpass, stabilizing on a plateau at a distance of around 3 km. This 3 km are not the distance since emission, as the plume is moved by the wind during the time from ship overpass to this point. Taking the combination of plume forward trajectories and simple Gaussian plume model, the plume age at this point is estimated to be ~400 seconds or ~6.5 minutes, in which the emitted air parcels traveled a distance of ~1.5 km. This is in the same order of magnitude than the measurements and model results discussed above.

To conclude, after a few minutes, at the latest after 10 minutes, the NO to NO_2 conversion reaches its steady state, depending on the ambient ozone concentration. As the plumes

[1] Middleton, D. R., Luhana, L. and Sokhi, R. S.: Review of methods for NO to NO2 conversion in plumes at short ranges, Environment Agency, Bristol., 2007.

[2] Meier, A. C.: Measurements of Horizontal Trace Gas Distributions Using Airborne Imaging Differential Optical Absorption Spectroscopy, phd thesis, University of Bremen, Bremen., 2018.

considered in the manuscript are usually older than 10 minutes, NO to NO_2 titration should not have a strong influence on the presented results. However, for a potential next step, the derivation of NO_x emission factors, accurate modeling of the NO-to-NO_2-titration would be important.

Regarding clouds: The following sentence was added to the manuscript: "In the following, only clear sky days or measurements under cloud free conditions are considered." and the whole paragraph was moved to Section 3.1.

As requested, a few words on possible error sources for the AirMAP measurements were also added.

Below, we reply point-by-point to the specific comments. As far as possible, we have considered the suggestions in the revised manuscript.

Specific points:

Page 2, Line 5: specify whether these are ship or land based in situ measurements

Both ship-borne and land-based in-situ measurements of shipping emissions are common. There are even airborne measurements, e.g. by Beecken et al. (2014)[3] and Balzani Lööv et al. (2014)[4].

Changed the sentence from

"Most measurements of pollution are performed with in-situ instrumentation, and this includes monitoring of the effect of ship emissions."

to

"Most measurements of **air** pollution are performed with in-situ instrumentation, and this includes monitoring of the effect of ship emissions, **which is usually performed with either land-based or shipborne in situ measurements.**"

Page 3, Section 2.1: Mention temporaral resolution of measurements here

We added the following sentences to Section 2.1:
"The total exposure time (or integration time) per measurement is 10 seconds for off-axis measurements and 20 seconds for zenith sky reference measurements. A new azimuthal measurement in one of the five different directions (see Section 2.2 and Fig. 1) starts about every 30 seconds. The measurement sequence is intermitted by a vertical scan in the main direction (335° azimuth) and a zenith sky measurement, both together taking in total around 90 seconds. The temporal resolution for one viewing direction, i.e. the time until the same azimuthal direction is probed again, is around 4 minutes. "

Page 4, Line 7: Not sure column amount is a concentration?

A column amount is not a concentration, but integrating a concentration along a certain light path delivers a column amount. Changed the structure of the sentence from "The quantity retrieved from DOAS measurements is the concentration of an absorber integrated along the atmospheric light path, the so-called slant column density (SCD)."

to

"The quantity retrieved from DOAS measurements is **the so-called slant column density (SCD), the integrated concentration of an absorber along the atmospheric light path.**"
to make it more precise.

3 Beecken, J., Mellqvist, J., Salo, K., Ekholm, J., and Jalkanen, J.-P.: Airborne emission measurements of SO2 , NOx and particles from individual ships using a sniffer technique, Atmos. Meas. Tech., 7, 1957-1968, https://doi.org/10.5194/amt-7-1957-2014, 2014.

4 Balzani Lööv, J. M., Alfoldy, B., Gast, L. F. L., Hjorth, J., Lagler, F., Mellqvist, J., Beecken, J., Berg, N., Duyzer, J., Westrate, H., Swart, D. P. J., Berkhout, A. J. C., Jalkanen, J.-P., Prata, A. J., van der Hoff, G. R., and Borowiak, A.: Field test of available methods to measure remotely SOx and NOx emissions from ships, Atmos. Meas. Tech., 7, 2597-2613, https://doi.org/10.5194/amt-7-2597-2014, 2014.

Page 8, Line 9: Not sure what you mean by “instrument measures in wind direction”

The whole sentence was reformulated to: “But as the movement of the ship together with the measured wind can result in an apparent wind direction very different from the measured wind direction, a measurement along the measured wind direction (windward, i.e. pointing anti-parallel to the wind vector) does not in general correspond to a measurement along the plume. ”

Page 8, Line 14: NO2 only increases up to a point…

Yes, of course, thanks for noticing. Corrected to:

“Therefore, the NO_2 signal increases **(up to a point)** with distance from the ship and, depending on the wind direction, with distance from the ship track.”

Page 11, Figure 6/7: In situ value colour saturates. Please mention what is the value in the text if not planning to change the colour scale. Maybe you could include it in Figure 5 as a function of time?

Good suggestion, as the information that the in situ instrument in fact measured two overlapping plumes got lost in the saturated color scale before. We included the measured in-situ values in the text and additionally pointed out that the in situ instrument measured two overlapping plumes.

Adding the in-situ curve to Figure 5, however, does not work, as the in-situ instrument measures much higher values, in this case for example reaching nearly 10 ppb and extending the y-axis range to account for the much higher in-situ values would substantially decrease the dynamics of the MAX-DOAS curves which is needed here for distinguishing the different cases.

Figures 6/7/8/9: I find the forward trajectory of the plumes a bit hard to interpret. What is the timescale on these? Do the black to grey values denote anything?

The lightness of the gray shading denotes the age of the plume. A colorbar showing the relationship between the lightness of the gray shading and the plume age was included in all plots showing modelled plumes.

Figure 10 and discussion in Section 5.3: I find the discussion of plume height a bit confusing and how it is used in the airborne observations. The MAX-DOAS on the tower seems to measure above the ship according to Figure 10, and the plume is not at the surface in the figure. Is there an assumed start height of the plume above the ocean?

As the MAX-DOAS measures down to the sea surface, the plume is assumed to reach down to the surface as well. The plume modelling supports this assumption. We added a hint on this to the text.

We also added the information that the heights are not to scale to the caption of Figure 10.

The AirMAP instrument is measuring the column to the surface. Why is 500 m used for the AMF calculation and not 335 m? Do the 335 m and 500 m height box profiles include a constant VMR to the surface? I don’t think different assumptions will change the results by much, but the description of profiles and relation to the figure could do with some clarity.

A 335m box profile could have been used, but only for this specific ship. The vertical extent of the other plumes in the figure are certainly different from this, probably larger, as the plumes are older. 500m seemed like a good first guess for all the ships. The correction to the measured/modeled plume height (here 335m or 320m, respectively) is done in the computation of the in plume VMR. And yes, the box profile assumes constant NO_2 up to 500m. We added this information to the manuscript and the respective paragraph now reads:

“For the retrieval of NO_2 vertical column densities, air mass factors were calculated for an NO_2 box profile **assuming constant NO_2** in the lowest 500 m, in an atmosphere without aerosols and for a constant surface reflectance of 0.05. **This box profile height is an educated guess on an upper limit for the typical vertical plume extent for older ship plumes, which the plume modeling has proven to be in the right order of magnitude.**”

Figures 11 and 14: Why show VMR and not DSCD for the MAX-DOAS here? Even though the DSCD is very diluted over a large area, it would at least put the measurements in the same units for easier visual comparison.

Granted, but the DSCD along the path difference, $\Delta DSCD = DSCD_{vis} - DSCD_{UV}$, is smaller than the DSCD along the UV path, $DSCD_{UV}$, and this reverses the situation in the figure: The higher NO_2 value is no longer shown along ΔL, where the plume is located, but close to the instrument along L_{UV}, and much lower NO_2 is shown along ΔL where the plume is. This is rather unintuitive, as shown below, so we would prefer to keep the plotted quantities as is.

Existing figure showing MAX-DOAS **VMR**:

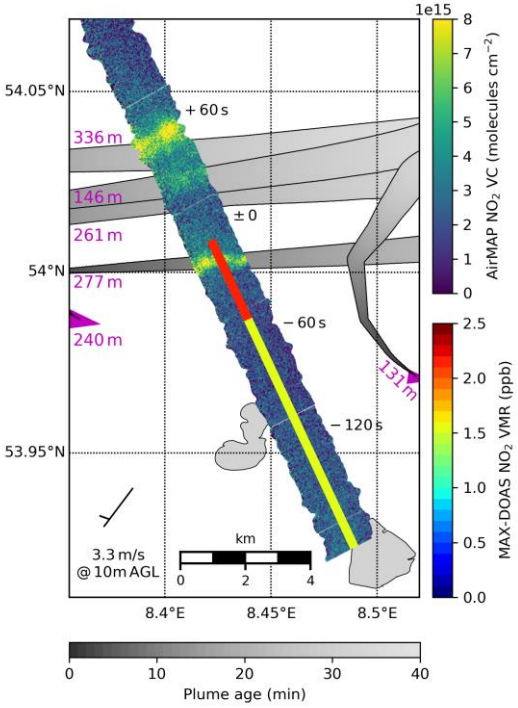

Figure showing MAX-DOAS **DSCD** instead:

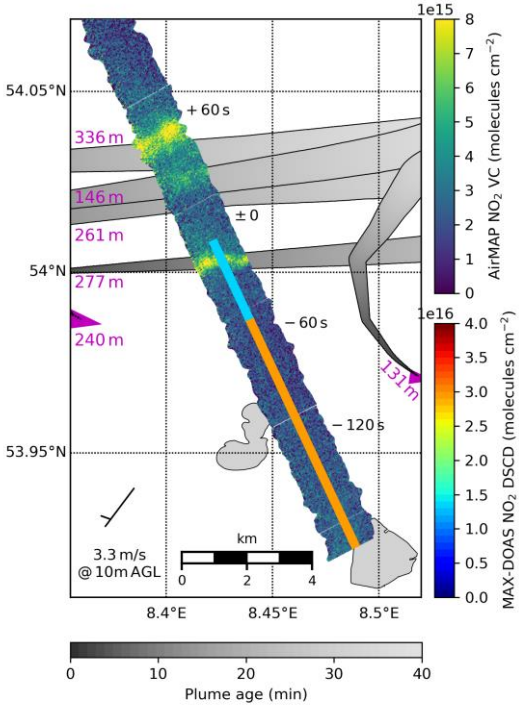

To better visually discriminate the two measurements, we changed the color-scale of the AirMAP measurements to *viridis*, one of the new perceptually uniform sequential colormaps introduced with *Python* package *Matplotlib* version 2.

Technical corrections:

Page 2, Line 14: change colon to semicolon

Done.

Page 3, Line 25 and 26: Change “in a” to “at a” in both cases

Done.

Page 13, Line 2: “lightboth” not a word

Changed “concentrations on all lightboth path segments” to

“concentrations on both path segments”

figure 10: change “not up to scale” to “not to scale”

Done.

Page 18, Line 3: change colon to semicolon

Done.

Interactive comment on Atmos. Meas. Tech. Discuss., doi:10.5194/amt-2018-348, 2018.

Studies of the horizontal inhomogeneities in NO_2 concentrations above a shipping lane using ground-based MAX-DOAS measurements and validation with airborne imaging DOAS measurements

André Seyler[1], Andreas C. Meier[1], Folkard Wittrock[1], Lisa Kattner[1,2], Barbara Mathieu-Üffing[1,2,a], Enno Peters[1,b], Andreas Richter[1], Thomas Ruhtz[3], Anja Schönhardt[1], Stefan Schmolke[2], and John P. Burrows[1]

[1]Institute of Environmental Physics, University of Bremen, Germany
[2]Federal Maritime and Hydrographic Agency (BSH), Hamburg, Germany
[3]Institute for Space Sciences, Freie Universität Berlin, Germany
[a]now at: State Agency for Agriculture, Environment and Rural Areas Schleswig-Holstein (LLUR), Germany
[b]now at: Institute for the Protection of Maritime Infrastructures, German Aerospace Center (DLR), Bremerhaven, Germany

Correspondence to: André Seyler (aseyler@iup.physik.uni-bremen.de)

Abstract.

This study describes a novel application of an "onion peeling" like approach to MAX-DOAS measurements of shipping emissions aiming at investigating the strong horizontal inhomogeneities in NO_2 over a shipping lane. To monitor ship emissions on the main shipping route towards the port of Hamburg, a two-channel (UV and visible) MAX-DOAS instrument was deployed on the island Neuwerk in the German Bight, 6–7 km south of the main shipping lane. Utilizing the fact that the effective light path length in the atmosphere depends systematically on wavelength, simultaneous measurements and DOAS retrievals in the UV and visible spectral range are used to probe air masses at different horizontal distances to the instrument to estimate two-dimensional pollutant distributions. Two case-studies have been selected to demonstrate the ability to derive the approximate plume positions in the observed area. A situation with northerly wind shows high NO_2 concentrations close to the measurement site and low values in the north of the shipping lane. The opposite situation with southerly wind, unfavorable for the on-site in situ instrumentation, demonstrates the ability to detect enhanced NO_2 concentrations several kilometers away from the instrument. ~~To validate the approach~~Using a Gaussian plume model, in-plume NO_2 volume mixing ratios can be derived from the MAX-DOAS measurements.

For validation, a comparison to ~~air-borne~~ airborne imaging DOAS measurements during the NOSE campaign in July 2013 is performed, showing good agreement between the approximate plume position derived from the onion peeling MAX-DOAS and the ~~air-borne measurements. Combining synergistically information about the plume width from the air-borne measurements and about the vertical plume extent from MAX-DOAS, yields NO_2 concentrations in the plume from both measurements which agree very well~~ airborne measurements as well as between the derived in-plume NO_2 VMRs.

1 Introduction

Over the last decades, there has been a strong increase in ship traffic and shipping emissions of gas phase pollutants but a reduction in their land sources in much of Europe. This has lead to an increasing contribution of shipping emissions to air pollution in coastal regions. Consequently, emission reduction measures ~~such as lowering~~ have been enacted by the International Maritime Organization (IMO) in the International Convention for the Prevention of Pollution from Ships (MARPOL 73/78 Annex VI) globally as well as, more stringent, locally in so-called emission control areas (ECAs) like North and Baltic Sea (IMO, 2009). To reduce sulfur oxides (SO_x) emissions, at the time of this study, the allowed sulfur content in shipping fuel ~~according to MARPOL VI (IMO, 2008) have been enacted in many places including the North Sea and the Baltic Sea~~is limited to 0.1 % in ECAs (since 2015, before: 1.0 %) and to 3.5 % globally, which is planned to be reduced to 0.5 % by 2020. For NO_x, the allowed emission rate depends on the rated rotational speed of the engine crankshaft (engine power and fuel efficiency) and is implemented in 3 tiers: Tier I (globally) for ships built between 2000 and 2010, Tier II (globally) for ships built from 2011 onwards and Tier III (locally in ECAs) for ships built from 2016 onwards, the last one not yet implemented in North and Baltic sea, shifted to 2021 (IMO, 2017). In order to monitor the effectiveness of these measures as well as the overall impact of ship emissions on air quality, measurements of air pollution from ships are required.

Most measurements of air pollution are performed with ~~in-situ~~ in situ instrumentation, and this includes monitoring of the effect of ship emissions, which is usually performed with either land-based or shipborne in situ measurements. As shown in Seyler et al. (2017), MAX-DOAS measurements can provide both a complementary approach and an alternative to ~~in-situ~~ in situ trace gas measurements at sites, where the ships are several kilometers away from the instrument and interpretation of ~~in-situ~~ in situ measurements is challenging due to dilution and broadening of the plume during the travel time from the ships to the measurement site.

MAX-DOAS measurements pointing at the horizon probe a long horizontal light path and are thus very sensitive to absorbers located close to the ground. The strong wavelength dependence of Rayleigh scattering ($\propto \lambda^{-4}$) leads to longer effective horizontal light paths for longer wavelengths. Simultaneous measurements and DOAS retrievals in the UV and visible spectral range can thus be used to probe different parts of the horizontal light path, an approach which is often called "onion peeling" method and has been applied to MAX-DOAS measurements before~~:~~; Ortega et al. (2015) used this method to retrieve two dimensional NO_2 fields from circular azimuth scans around the instrument in the framework of the MAD-CAT campaign (Multi-Axis DOAS Comparison campaign for Aerosols and Trace gases) in Mainz, Germany. The aim of the study was the investigation of horizontal gradients in a strongly polluted urban area, with the cities of Mainz, Wiesbaden and Frankfurt as well as the Frankfurt airport close by, focussing on comparison to satellite measurements.

The present study focuses on measurements in a relatively clean coastal region where ships passing by the island are often the only dominant source of air pollution (Seyler et al., 2017). The ships are mobile point sources of NO_x emissions and the emitted exhaust gas plumes are transported, depending on wind conditions, leading to a strongly inhomogeneous NO_2 field over the shipping lane.

Ortega et al. (2015) probed a circular area with 14 azimuthal viewing directions distributed over a 360° view around the instrument. In the present study, a similar measurement pattern was applied using 5 different azimuth directions distributed over a 120° angle to cover the shipping lane close to the island (see Fig. 1b) with sufficient time resolution to monitor individual passing ships. The onion peeling approach provides additional distance information for the measured NO_2 columns.

This study uses measurements in both the UV (∼350 nm) and blue spectral range (∼450 nm), while Ortega et al. (2015) used additional measurements in the yellow spectral range (∼570 nm) to get an even longer effective horizontal light path and cover a larger region. This is not possible here as the instrument used has a smaller wavelength coverage.

As can be seen from Fig. 1a and b, the measurement site on the island Neuwerk is ideal for applying this measurement principle: The distance between site and shipping lane is ~~on~~ of the order of 6 to 10 kilometers, depending on the azimuthal viewing direction, which is in the range of typical UV horizontal effective light path lengths (Seyler et al., 2017). Depending on the azimuthal direction, the additional probing distance gained by measurements in the visible spectral range covers the shipping lane or the region in the north of the ship track. As it is shown in the following, this enables the NO_2 distribution caused by the ship emission plumes over and around the ship track to be determined. In addition even the distance and course of the emitted plumes is observed.

This publication is a follow up to an earlier study entitled "Monitoring shipping emissions in the German Bight using MAX-DOAS measurements" (Seyler et al., 2017) where long-term measurements were used to asses the impact of shipping emissions on the regional air quality, while the present study focuses on describing, demonstrating and validating a new method for improved measurements of ship emissions and their localization.

The present study is part of the project MESMART (measurements of shipping emissions in the marine troposphere), a cooperation between the University of Bremen (Institute of Environmental Physics, IUP) and the German Federal Maritime and Hydrographic Agency (Bundesamt für Seeschifffahrt und Hydrographie, BSH), supported by the Helmholtz Zentrum Geesthacht. For further information visit http://www.mesmart.de/.

2 Measurement site and instrumentation

2.1 MAX-DOAS instrument

The multi axis differential optical absorption spectroscopy (MAX-DOAS) (Hönninger et al., 2004; Wittrock et al., 2004) is a well-established technique for measurements of trace gases that absorb in the UV and visible spectral range. This passive remote sensing method measures spectra of scattered sunlight in multiple viewing directions and is highly sensitive to absorbers in the atmospheric boundary layer. A two-channel MAX-DOAS instrument was deployed on the island Neuwerk from July 2013 to July 2016. It comprises a telescope unit with a field of view of 1° on a pan-tilt head, an optical fiber cable and two spectrometers with CCD cameras for UV (304.6–371.7 nm) and visible (398.8–536.7 nm) spectral range. This arrangement is optimized for the simultaneous retrieval of NO_2 and O_4 in both spectral domains. The total exposure time (or integration time) per measurement is 10 seconds for off-axis measurements and 20 seconds for zenith sky reference measurements. A new azimuthal measurement in one of the five different directions (see Section 2.2 and Fig. 1) starts about every 30 seconds. The

Table 1. DOAS fit settings for the retrieval of NO_2 and O_4 in UV and visible spectral range

Parameter	NO_2 (UV)	NO_2 (visible)
Fitting window	338–370 nm	425–497 nm
Polynomial degree	4	3
Intensity offset	Constant	Constant
Zenith reference	Coinciding zenith measurement*	Coinciding zenith measurement*
SZA limit	Up to 85° SZA	Up to 85° SZA
O3	223 K & 243 K (Serdyuchenko et al., 2014)	223 K (Serdyuchenko et al., 2014)
NO_2	298 K (Vandaele et al., 1996)	298 K (Vandaele et al., 1996)
O_4	293 K (Thalman and Volkamer, 2013)	293 K (Thalman and Volkamer, 2013)
H2O	–	293 K (Lampel et al., 2015)
HCHO	297 K (Meller and Moortgat, 2000)	–
Ring	SCIATRAN (Rozanov et al., 2014)	SCIATRAN (Rozanov et al., 2014)

* Interpolation in time between the zenith measurements directly before and after the off-axis scan.

measurement sequence is intermitted by a vertical scan in the main direction (335° azimuth) and a zenith sky measurement, both together taking in total around 90 seconds. The temporal resolution for one viewing direction, i.e. the time until the same azimuthal direction is probed again, is around 4 minutes.

A detailed description of the MAX-DOAS instrument and its components as well as the general measurement geometry for ship emission measurements is given in Seyler et al. (2017). Details of the DOAS fit settings used are ~~given~~ summarized in Table 1.

2.2 Measurement site

Neuwerk is a small island in the German Bight, northwest of the city of Cuxhaven at the mouth of the river Elbe, around 9 kilometers off the coast. An overview of the area is shown in Fig. 1a. The main shipping lane into the river Elbe towards the port of Hamburg passes the island in the north ~~in~~ at a distance of 6–7 km (see Fig. 1a). The MAX-DOAS instrument was installed on a radar tower ~~in~~ at a height of 30 meters above ground level. Additional instrumentation on site included in situ gas analyzers (NO_x, SO_2, O_3, CO_2) in a combined compact housing (Airpointer from MLU-recordum, Austria), a Davis Vantage Pro 2 semi-professional weather station and an automatic identification system (AIS, (IMO, 2002)) receiver. The AIS signal broadcasts various information like identification, position, speed, course and size of the ship. Broadcasting equipment is mandatory for all ships larger than 20 m. In the present study, the AIS information is used to attribute the measurements to individual ships. Wind direction and speed is available with a time resolution of 10 minutes from two stations (see Fig. 1a), one on Neuwerk and one on the neighboring island Scharhörn, operated by the Hamburg Port Authority (HPA).

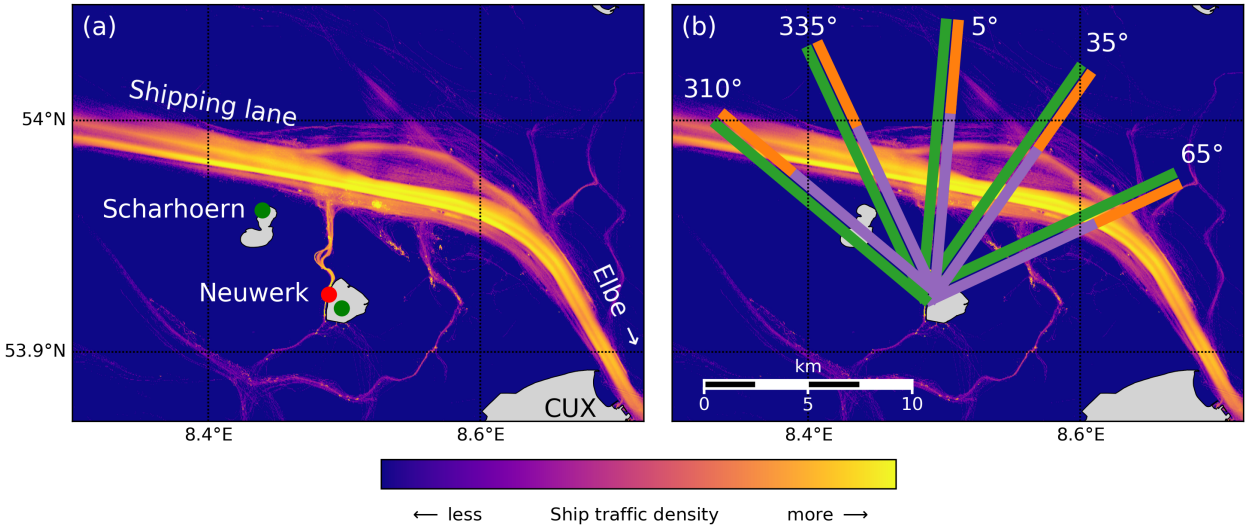

Figure 1. (a) Ship traffic density map calculated from all received AIS messages (2013-2016) showing the main shipping lane from the North sea into the Elbe river close to the measurement site on a radar tower on the island Neuwerk (red dot). Wind measurements are available on Neuwerk as well as the ~~neighbouring~~ neighboring island Scharhörn (green dots). (b) Effective horizontal light paths in UV (purple line) and visible spectral range (green line) for the five azimuthal viewing directions of the MAX-DOAS instrument (310°, 335°, 5°, 35°, 65°, with respect to north), shown for typical light path lengths of 9 km (UV) and 13 km (vis), respectively. The difference between both paths, ΔL, is highlighted by the orange line.

To sample a larger region, the MAX-DOAS was set up to have five different azimuthal viewing directions: 310°, 335°, 5°, 35° and 65° with respect to north, each pointing towards different sections of the shipping lane (see Fig. 1b).

For further information on the measurement site and instrumentation see Seyler et al. (2017).

3 Methodology

The quantity retrieved from DOAS measurements is the so-called slant column density (SCD), the integrated concentration of an absorber ~~integrated~~ along the atmospheric light path~~, the so-called slant column density (SCD)~~. To measure the NO_2 absorption inside the ship plumes emitted on the shipping lane, the instrument is pointing in 0.5° elevation towards the horizon. Taking a close-in-time zenith-sky measurement as a reference, in a first assumption only the absorption along the horizontal part of the effective light path is retrieved and the absorption higher up in the atmosphere cancels out. This yields the differential slant column density (DSCD).

For the comparison with in situ measurements the MAX-DOAS horizontal trace gas columns are converted to horizontal path averaged volume mixing ratios (VMR) by using the O_4 scaling approach (see Section 3.1). The onion peeling approach

(see Section 3.2) is used to separate NO_2 absorptions at different horizontal distances to derive separate NO_2 VMRs and estimate the distance to the plumes.

3.1 O_4 scaling approach – methodology and limitations

The oxygen collision complex O_4 absorbs in similar wavelength ranges as NO_2 in the UV and visible. Since the near-surface concentration of O_4 is known, the effective horizontal path length can be calculated by dividing the DSCD of O_4 by its number density n_{O_4}:

$$L = \frac{\mathrm{SCD}_{O_4,\mathrm{horiz}} - \mathrm{SCD}_{O_4,\mathrm{zenith}}}{n_{O_4}} = \frac{\mathrm{DSCD}_{O_4}}{n_{O_4}}$$

$$L = \frac{\mathrm{SCD}_{O_4,\mathrm{horiz}} - \mathrm{SCD}_{O_4,\mathrm{zenith}}}{n_{O_4}} = \frac{\mathrm{DSCD}_{O_4}}{n_{O_4}} \quad (1)$$

with $n_{O_4} = (n_{O_2})^2$, which can be calculated from the measured temperature and pressure. This can be done independently for both UV and visible measurements, giving average light path lengths of $L_{\mathrm{UV}} = (9.3 \pm 2.3)\,\mathrm{km}$ and $L_{\mathrm{vis}} = (12.9 \pm 4.5)\,\mathrm{km}$ [mean $\pm$ standard deviation] for the three years of measurements on Neuwerk, depending on the observational conditions. Under clear sky conditions, typical light path lengths are 10 km in the UV and 15 km in the visible spectral range (Seyler et al., 2017).

Knowing the horizontal light path length L, the NO_2 DSCD can be divided by L to obtain the average concentration (number density) of NO_2 along the horizontal light path. Dividing the NO_2 concentration by the concentration of air, n_{air}, which can be calculated via the ideal gas law from the measured temperature and pressure, yields the average volume mixing ratio (VMR) along L:

$$\mathrm{VMR}_{NO_2} = \frac{\mathrm{SCD}_{NO_2,\mathrm{horiz}} - \mathrm{SCD}_{NO_2,\mathrm{zenith}}}{L \cdot n_{\mathrm{air}}} = \frac{\mathrm{DSCD}_{NO_2}}{L \cdot n_{\mathrm{air}}}$$

$$\mathrm{VMR}_{NO_2} = \frac{\mathrm{SCD}_{NO_2,\mathrm{horiz}} - \mathrm{SCD}_{NO_2,\mathrm{zenith}}}{L \cdot n_{\mathrm{air}}} = \frac{\mathrm{DSCD}_{NO_2}}{L \cdot n_{\mathrm{air}}} \quad (2)$$

This ~~O4~~ O_4 scaling approach has been successfully applied to MAX-DOAS measurements before, for example in urban polluted areas (Sinreich et al., 2013; Wang et al., 2014) or at high mountain sites (Gomez et al., 2014; Schreier et al., 2016).

For a homogeneous, well-mixed NO_2 field along the light path, this VMR must agree with in situ measurement from the same altitude. For the ship emission case, where emission plumes are filling only a small fraction of the several kilometers long light path, the path-averaged MAX-DOAS VMR will not represent the VMR inside the plume and values will be smaller than in situ measurements inside the plume (Seyler et al., 2017).

~~However~~In addition, the different shapes of the atmospheric profiles of NO_2 (emitted and formed close to the surface) and O_4 (exponentially decreasing with altitude) introduce systematic errors as has been shown by Sinreich et al. (2013) and Wang et al. (2014). To account for this, correction factors calculated by radiative transfer simulations are needed. These depend on well-known quantities such as solar zenith angle (SZA) and relative solar azimuth angle (RSAA) as well as on unknown quantities such as aerosol optical density (AOD), height of the NO_2 box profile and the extent and vertical position of the aerosol layer relative to the NO_2 profile (Sinreich et al., 2013), which are not measured and cannot be easily approximated for the present study. In previous studies, it has been assumed that NO_2 is well mixed within a layer from the surface up to a top layer height and absent above this altitude. This is not a valid assumption in case of horizontally inhomogeneous NO_2 fields such as those probed over the shipping lane. As in Seyler et al. (2017), scaling factors are therefore not considered here, presumably leading to a systematic overestimation of path lengths and thus underestimation of MAX-DOAS VMRs (Sinreich et al., 2013; Wang et al., 2014).

Clouds can decrease or increase the light path length (and O_4 absorption) by multiple scattering, depending on the cloud's position and its optical properties, especially its optical thickness (Wagner et al., 2014). As a result, a day with scattered or broken clouds will show much more variation in path lengths than a clear sky day, even between consecutive measurements, by having clouds in either off-axis or reference measurement or both or neither, which makes interpretation of results more difficult. In the following, only clear sky days or measurements under cloud free conditions are considered.

3.2 "Onion peeling" MAX-DOAS approach

As mentioned above, the wavelength dependence of Rayleigh scattering results in a wavelength dependence of the light path lengths after the last scattering point. This can be utilized to probe different air masses in the atmosphere by measuring both in the UV and visible spectral range.

The aforementioned O_4 scaling method gives two path-averaged volume mixing ratios for each measurement; one for the shorter UV and one for the longer visible effective horizontal light path, which are shown in Fig. 1b and 2 as a purple and green line, respectively. One can calculate a third volume mixing ratio from the difference of the two DSCDs and path lengths:

$$\mathrm{VMR}_{@\Delta L} = \frac{\mathrm{DSCD}_{\mathrm{vis}} - \mathrm{DSCD}_{\mathrm{UV}}}{(L_{\mathrm{vis}} - L_{\mathrm{UV}}) \cdot n_{\mathrm{air}}} = \frac{\Delta\mathrm{DSCD}}{\Delta L \cdot n_{\mathrm{air}}} \tag{3}$$

This yields the average volume mixing ratio $\mathrm{VMR}_{@\Delta L}$ along the path difference ΔL, which is shown as an orange line in Fig. 1b and 2.

As each ship is a moving point source for NO_2 emissions, the NO_2 field over a shipping lane is strongly inhomogeneous. This means that the NO_2 is in general not distributed evenly along any of the effective horizontal light paths.

Depending on the position of the plume in relation to the UV and visible light path, the path averaged mixing ratios can differ substantially. Figure 2 shows schematically the plume-light-path geometry for three possible observation scenarios and illustrates the expected NO_2 signal for the different horizontal light paths.

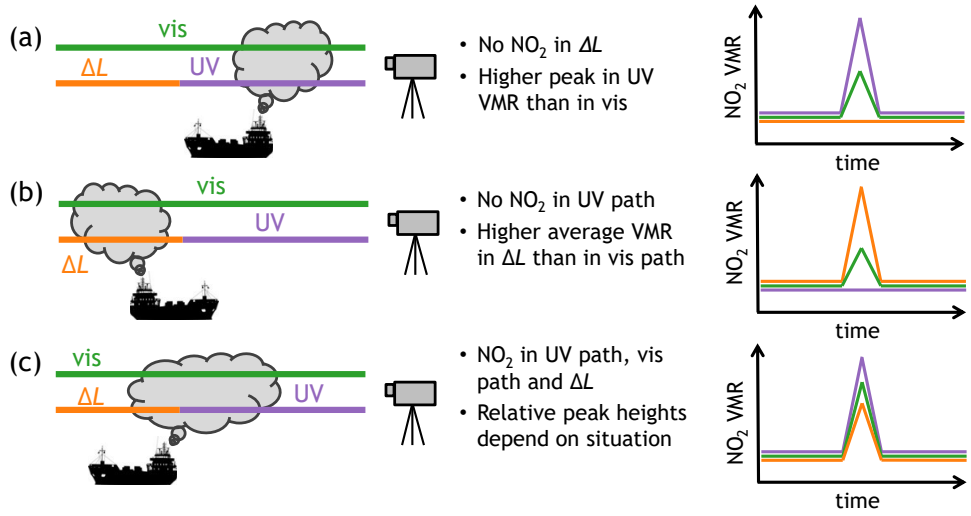

Figure 2. Plume–light-path geometry and the resulting path averaged NO_2 concentrations for three possible cases: When the plume is close to the instrument and completely covered by the UV path (a), when the plume is further away from the instrument than the UV scattering point and is only covered by the visible path (and ΔL) (b) and when the plume is located around the UV scattering point (c)

In case (a) the plume is close to the instrument and is completely covered by the shorter UV path L_{UV}, i. e. it is closer to the instrument than the (mean) last scattering point in the UV. Although both paths cover the same amount of NO_2, the retrieved path-averaged concentration is higher for the UV signal because of the higher relative contribution of the fraction of the light path which probes the NO_2 plume. The path difference ΔL incorporates no NO_2 from the emission plume, resulting in zero or background level NO_2 from there. It can be seen from Fig. 1b that this situation occurs for northerly wind directions. Section 4.2 shows example measurement results for such a case.

Case (b) shows the opposite situation, when the plume is further away from the instrument than the UV scattering point and only covered by the visible path L_{vis}. This results in an enhanced signal for the NO_2 retrieved in the visible, and no signal in the UV. The path averaged concentration retrieved for ΔL is even higher, because ΔL is only a segment of the visible path and therefore shorter than the complete visible path. On Neuwerk, such a situation can occur for southerly winds (compare Fig. 1b). Section 4.3 shows example measurement results for this kind of situation.

In case (c) the plume is close to the UV scattering point. All three light paths see enhanced NO_2. The relative peak heights depend on the fraction of plume NO_2 probed by the different light paths as well as the total light paths lengths. ~~Situations~~ On Neuwerk, situations like this will most likely occur for westerly and easterly winds.

As already discussed in Seyler et al. (2017), the measured column density as well as the path-averaged concentration do not only depend on the emitted amount of NO_2 inside the plume, but also on the angle of intersection between plume and line

of sight of the instrument. The smallest absorptions, and thus column amounts, will be retrieved if the plume runs ~~orthogonal~~ orthogonally to the line of sight, the highest values if the instrument measures along the plume. The latter can occur for certain combinations of wind direction ~~, wind~~ and speed and ship movement direction and speed. ~~Because of~~ But as the movement of the ~~ships (and the shape of the shipping lane), this is in general not the case when the instrument measures in wind direction , as it would be for a stationary point source~~ship together with the measured wind can result in an apparent wind direction very different from the measured wind direction (Berg et al., 2012), a measurement along the measured wind direction (windward, i.e. pointing anti-parallel to the wind vector) does not in general correspond to measurements along the plume.

The time span between plume emission and measurement is ~~also~~ important for the measured ~~NO_2~~ NO_2 values because of NO to ~~NO_2 titration~~ NO_2 titration in the plume ($NO + O_3 \rightarrow NO_2 + O_2$), as a large fraction of nitrogen oxides (NO_x) is emitted as NO (Alföldy et al., 2013; Zhang et al., 2016), which does not absorb in the spectral range covered and cannot be measured with MAX-DOAS. Therefore, the ~~NO_2 signal increases~~ NO_2 content in the plume is expected to increase with distance from the ship ~~and,~~ until a steady state is reached. Middleton et al. (2007) modeled the NO to NO_2 conversion in plumes at short ranges depending on the ~~wind direction, with~~ O_3 concentration. For O_3 VMRs of 30 to 50 ppb (20 to 70 ppb), which are typically measured at our Neuwerk station in summer, they predicted the steady state to be reached after 3 to 4 minutes and in the steady state the fraction of NO_2 on the overall NO_x to be 65–70 %. For very fresh plumes shortly after emission, Alföldy et al. (2013) found that the NO_2-to-NO_x ratio in the plume does not depend on ambient ozone concentrations, as diffusion limits the availability of O_3. Airborne imaging DOAS measurements during an overflight over a ship and its plume from the NOSE campaign on 21 August 2013 presented by Meier (2018) show an increase in NO_2 with flown distance from the ship ~~track~~overpass. After the airplane covered a distance of around 3 km the values stabilize and do not increase further. Applying the plume modeling approach discussed in Section 3.3, the plume age at this point where presumably the steady state was reached was estimated to be around 6.5 minutes, in which the respective plume air parcel traveled a distance of ~ 1.5 km. Other, unpublished in situ measurements of ship plumes indicate that after 8–10 minutes at the latest the plume NO content is below 20–30 % for all ships. In view of these findings, as the plumes investigated in our study are mostly older than 10 minutes, we expect and assume the steady state to be already reached.

The lifetime of NO_2 is on the order of several hours, but as the time scales investigated here are shorter, we expect the influence to be small.

3.3 Plume trajectories and plume modeling

~~Here,~~ For a more quantitative treatment of the ship emissions, the exhaust plumes and their movement over time need to be considered. Here, ship plume trajectories have been calculated as simple forward trajectories ~~on~~ combined with a Gaussian plume model. On a 10 s time grid, ~~where~~ at each time step, each point shaped plume air parcel ~~on each time step~~ is moved from its old position to a new position, ~~depending~~ which depends on wind direction and speed. Each ship emits a new plume air parcel ~~at each~~ per time step at the ~~actual ship position~~respective ship position, thus creating a chainline-like string of plume air parcels. By starting with an initialization period of ~~90 minutes before the measurements~~3 hours before the respective measurement time, old plumes from ships that passed by the island before and already left the ~~map~~ region of interest can

be included in maps as those shown in Fig. 4. ~~The width of the schematic plumes in the maps is not to scale and depends simply on the ship size, with broader plumes drawn for larger ships. Plume broadening and dilution over time is neglected. However, the gray shading of the drawn plumes gets brighter with each time step to indicate the plume age. The trajectories are two-dimensional, vertical wind components were not measured and are therefore neglected. While some weather models provide such vertical wind components, their spatial and time resolution is too low for this application~~

Plume broadening and dispersion over time is accounted for by modeling the width and height of the plumes with a Gaussian plume model (Pasquill, 1961; Gifford, 1961), an often used model for point source emitters like power plants. It describes the vertical and horizontal plume dispersion with two Gaussian curves and links the pollutant emission rate Q, the mean wind speed U (in x-direction) and the horizontal and vertical dispersion coefficients σ_y and σ_z to the concentration C at the point (x, y, z):

$$C(x,y,z) = \frac{Q}{2\pi U \sigma_y \sigma_z} \exp\left(\frac{-y^2}{2\sigma_y^2}\right) \exp\left(\frac{-(z-H)^2}{2\sigma_z^2}\right) \tag{4}$$

Where the vertical coordinate z is corrected for the effective stack height H (the effective height of the plume center line), the sum of the stack height and the initial plume rise.

The dispersion coefficients σ_y and σ_z are the standard deviations of the Gaussian shaping functions and depend on atmospheric stability. A simple classification scheme defining six different stability classes ranging from very unstable (A) to stable (F) based on wind speed and solar insolation (Pasquill, 1961) is shown in Tab. 2. One set of empirical functions for the dispersion coefficients σ_y and σ_z as functions of the along wind distance x is given by Martin (1976):

$$\sigma_y(x) = a \cdot x^{0.894} \tag{5}$$

and

$$\sigma_z(x) = c \cdot x^d + f \tag{6}$$

where the distance from the source x is input in kilometers to retrieve σ in meters. The stability-dependent empirical constants a, c, d, and f are given in Tab. 3, partially with a distinction between $x \leq 1\,\mathrm{km}$ and $x > 1\,\mathrm{km}$ (Martin, 1976).

As the ships are moving point sources, the course of the plume does not only depend on the wind direction but also on the previous pathway of the ship. The ships move with with a certain direction and speed, thus creating an apparent wind (Berg et al., 2012). It is therefore not sufficient to run the Gaussian plume model for each ship position on each timestep, it has to be combined with the simple forward trajectories, as each plume air parcel has been emitted at a different location. This is done by running the Gaussian plume model for the respective stability class that fits the prevailing weather conditions and creating look-up-tables (LUT) for the plume width and height depending on the distance from the emission point. For each plume air parcel in the trajectory this LUT is then evaluated at the distance this plume parcel traveled since its emission, to retrieve the plume width at this location. The plume width and height LUTs are gained from the Gaussian plume model by

Table 2. Atmospheric stability classification scheme (Pasquill, 1961; Turner, 1970) based on surface wind speed and solar insolation: A–very unstable, B–moderately unstable, C–slightly unstable, D–neutral. The additional stability classes E–slightly stable and F–stable occur only at night. For A–B take average of stability parameters (Tab. 3) for A and B.

Wind speed (10 m AGL) in m/s	Solar insolation		
	Strong	Moderate	Slight
< 2	A	A–B	B
2–3	A–B	B	C
3–5	B	B–C	C
5-6	C	C–D	D
> 6	C	D	D

going through every x distance in 10 meter steps (a 10 by 10 meter grid is used) and checking in across-wind direction in which distance from the plume centerline the concentration drops under a certain threshold level (in this study: 1/e) compared to the maximum concentration at the plume centerline at this respective x distance. By introducing this kind of normalization, the exact values of the multiplicative factors Q (emission rate) and U (wind speed) become irrelevant for the computation. For the plume width this LUT can be applied to all ships, but for the plume height, as this depends on the stack height, the LUTs have to be computed for each individual ship separately, as their stack heights differ. As neither ship height nor stack height is contained in the broadcasted AIS data, the stack height has to be researched for each ship individually. In this study it was estimated from pictures of a ship by comparing the stack height to the standardized height of the loaded containers. This is not so much of a problem here, as the plume height plays no role for the visual representation of the plumes in the maps (as they represent an aerial view) but only for the detailed analysis of specific plumes of specific ships.

For the method for deriving in plume NO_2 VMRs from MAX-DOAS (and airborne imaging DOAS) measurements described in Section 4.1, knowledge of the plume width (and height) is sufficient, so the concentration or emission rate is not modeled here. Plume chemistry like NO to NO_2 titration and NO_2 loss reactions/NO_2 lifetime is neglected. Another source of uncertainty is the fact that the Gaussian plume model only describes an average plume. Each snap-shot in time of a real plume will in general not look like a Gaussian plume, but if multiple snap-shots are averaged over a certain time period, the average shape should approach a Gaussian plume shape. Using the Gaussian plume model for the plume trajectories is therefore only an approximation.

4 Results

4.1 Onion peeling approach applied to ship emission measurements

Table 3. Empirical stability parameters for the computation of the horizontal and vertical dispersion coefficients σ_y, σ_z (Martin, 1976) for the different atmospheric stability classes according to Pasquill (1961). For intermediate stability classes like A–B, averages of parameter values for A and B are taken.

			$x \leq 1\,\mathrm{km}$			$x > 1\,\mathrm{km}$		
Stability class	Description	a	c	d	f	c	d	f
A	Very unstable	213	440.8	1.941	9.27	459.7	2.094	-9.6
B	Moderately unstable	156	106.6	1.149	3.3	108.2	1.098	2.0
C	Slightly unstable	104	61.0	0.911	0	61.0	0.911	0
D	Neutral	68	33.2	0.725	-1.7	44.5	0.516	-13.0
E	Slightly stable	50.5	22.8	0.678	-1.3	55.4	0.305	-34.0
F	Stable	34	14.35	0.740	-0.35	62.6	0.180	-48.6

~~Figure ??~~ Panel a in Fig. 3 shows the measured NO_2 DSCDs in 0.5° elevation for the 335° azimuth direction (compare Fig. 1b) on 26 May 2014. The NO_2 shows sharp peaks, which originate from shipping emissions, with rapid changes of NO_2 levels between consecutive measurements of up to one order of magnitude. The small, but non-zero baseline between the peaks shows an ambient NO_2 pollution, which is enhanced in the morning hours. The background NO_2 signal may be originating from land-based sources but may also contain residual, diluted shipping emissions. The morning enhancement might be due to the morning traffic rush hour or boundary layer height changes.

As a result of the longer light path, the NO_2 columns measured in the visible range are larger than in the UV. The difference between visible and UV columns, ΔDSCD, shows concurrent peaks for some of the ~~peaks~~cases, with varying relative height. The peak at 12:50 UTC is not visible in the ΔDSCD, indicating that the plume must be closer to the instrument than the UV scattering point.

~~Figure ??~~

Panel (b) in Fig. 3 shows the corresponding effective horizontal light path lengths derived from the measured O_4 DSCDs. For a clear sky day like this, path lengths are quite constant over time. ~~Clouds can decrease or increase the light path length (and O_4 absorption) by multiple scattering, depending on the cloud's position and its optical properties, especially its optical thickness (Wagner et al., 2014). As a result, a day with scattered or broken clouds will show much more variation in path lengths even between consecutive measurements by having clouds in either off-axis or reference measurement or both or neither, which makes interpretation of results more difficult.~~

~~Effective horizontal light path lengths on 26 May 2014 in 0.5° elevation and 335° azimuth for UV (purple) and visible spectral range (green) and their difference (orange)~~

~~Figure ??~~ Panel c in Fig. 3 shows the horizontal path averaged NO_2 volume mixing ratios retrieved from the NO_2 DSCDs by using the O_4 scaling approach with the path lengths for UV and visible shown in ~~Fig. ??~~Panel b, as well as the volume mixing ratio on the path difference calculated via Eq. 3. The baselines of all three curves agree very well, showing that the

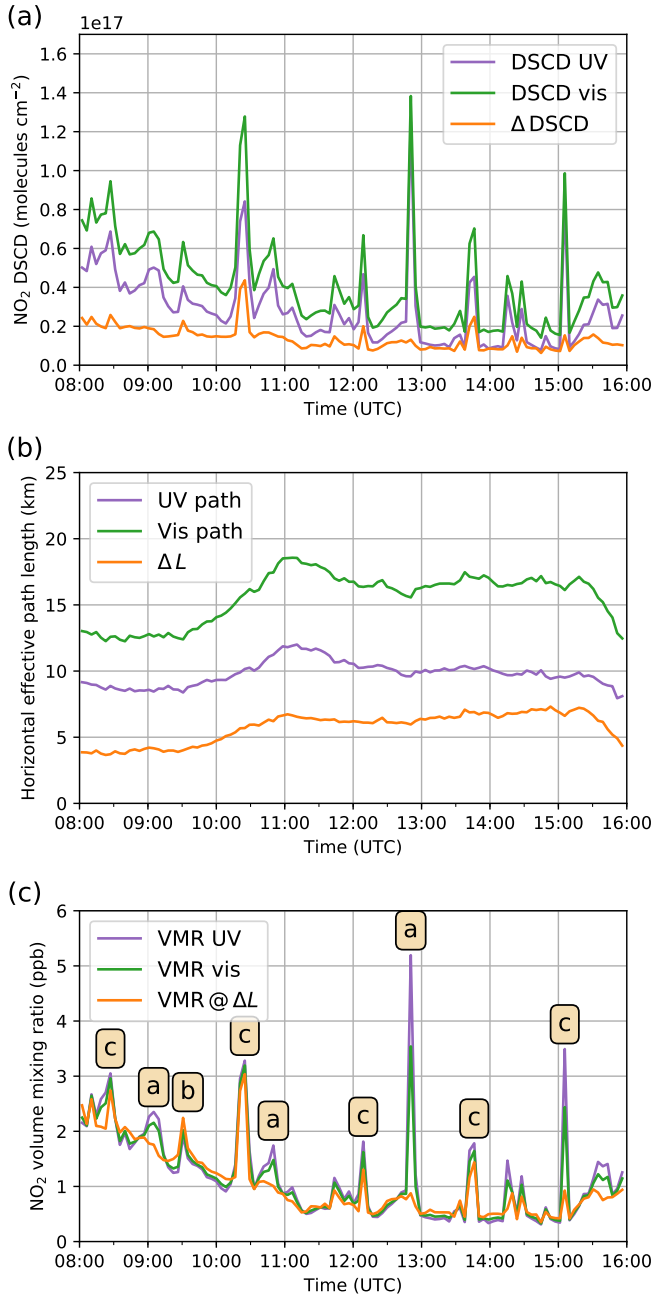

Figure 3. Differential slant column densities of NO_2 (a), horizontal effective path lengths (b) and horizontal path averaged volume mixing ratios of NO_2 on 26 May 2014 in 0.5° elevation and 335° azimuth for the UV (purple) and visible spectral range (green) and their difference (orange)

ambient NO_2 background pollution is well-mixed in the boundary layer and homogeneously distributed along all light paths sections. However, the sharp peaks originating from ship emission plumes have different relative heights, showing that the corresponding NO_2 field is inhomogeneous. The strong NO_2 signal at 12:50 UTC without enhanced NO_2 VMR on the path difference, resembling situation (a) in Fig. 2, will be further investigated in the next section.

~~Horizontal path averaged volume mixing ratios of NO_2 on 26 May 2014 in 0.5° elevation and 335° azimuth for the UV (purple) and visible path (green) as well as for the path difference ΔL (orange). The yellow labels over the peaks indicate the respective situation from Fig. 2.~~

4.2 Northerly wind situations

For northerly winds, the pollution plumes emitted from the ships are blown towards the radar tower, resulting in enhanced NO_2 concentrations south of the shipping lane (compare Fig. 1b). In the north of the shipping lane, concentrations should be low, resembling situation (a) in Fig. 2.

In Fig. 4, a 12 minute sequence of consecutive MAX-DOAS measurements on 26 May 2014 starting at 12:46 UTC (14:46 local time) is shown for more detailed investigation of the strong NO_2 signal already seen in Fig. ~~??~~ 3c at 12:50 UTC. Plotted in each map are the length and location of the UV path and ΔL as colored lines, with color representing the respective path averaged NO_2 VMR. In situ NO_2 VMRs are shown as colored dots at the measurement site. ~~Shown are also~~ Also shown are ship positions and course from AIS data, plume trajectories (see Section 3.3) and wind speed and direction measured by the weather station on Neuwerk.

The sequence of maps shows two ships (magenta triangles) on the shipping lane, moving in opposite directions. The larger ship (length 351 m) moves westward, the smaller ship (length 151 m) moves eastward. The locations of the two plumes (gray shaded stripes) differ considerably due to the different movement directions of the ships and the curved shape of the shipping lane around the island.

For the plume modeling, the stability class C representing slightly unstable conditions has been chosen based on the wind speed and the strong solar insolation on this clear sky day.

In the first panel, the MAX-DOAS measurements at 12:46:24 UTC in 335° azimuth direction are shown. The horizontal path averaged NO_2 VMRs are low (< 1 ppb NO_2) and agree very well between the different path segments as well as with the in situ measurements, showing that the ambient background NO_2 is homogeneously well-mixed in the boundary layer. The fact that the plume from the smaller ship shows up only slightly in the measurements ~~can have two possible reasons: Either the in-plume NO_2 concentrations are rather low or the plume is in the wrong height and not in the observed air volume along the line of sight of the instrument, which due to the 1° field of view is quite narrow close to the instrument.~~ might be due to low emissions from this comparatively small ship and the dilution of the already strongly dispersed plume, as the plume model predicts a vertical extent of the plume of ~ 400 m and a plume width of 1200–1300 m at a plume age of 700-800 seconds.

Panels 2 to 4 (5°, 35° and 65° azimuth, respectively) show enhanced NO_2 VMRs (up to 4 ppb) along the UV path close to the instrument, likely due to the plume of the big ship, and low VMRs along ΔL further away from the instrument. Although

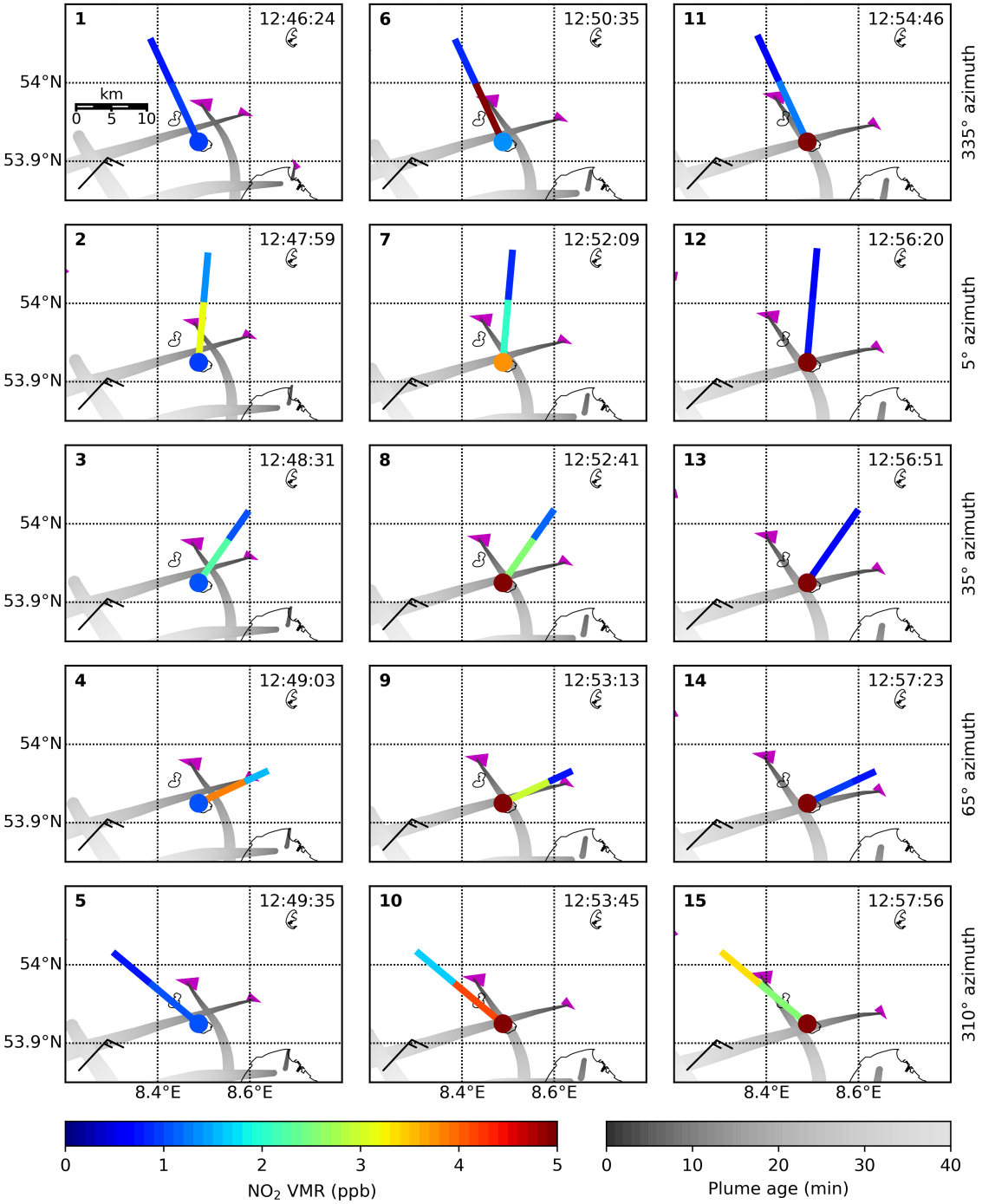

Figure 4. Sequence of maps showing 15 consecutive measurements in 0.5° elevation on 26 May 2014, starting at 12:46 UTC (14:46 local time): The extent of the UV path and ΔL and corresponding path averaged NO_2 VMRs are shown as colored lines. In situ NO_2 VMRs are shown as a colored dot at the location of the measurement site. Magenta triangles show the ship position and course (sharp tip), with larger triangles for larger ships. ~~Grey point clouds show forward trajectories~~ The modeled plumes are shown in gray, the lightness of the ~~emission plumes calculated from wind speed and direction for~~ gray shading representing the ~~moving ship~~plume age. Wind direction and speed is shown with meteorological wind barbs.

MAX-DOAS measurements show enhanced NO_2 between site and UV scattering point the plume has not reached the radar tower yet and in situ values therefore stay low.

Panel 5 shows the measurements in the 310° viewing direction which are similar to the measurements in 335° azimuth angle in Panel 1.

In Panels 6 to 10, the plume approaches the radar tower and in situ values begin to rise. MAX-DOAS VMRs are again high close to the radar tower and low in the north of the shipping lane. Due to different angles of intersection between plume and line of sight, the MAX-DOAS path averaged UV VMR is different, showing the highest value of ~ 5 ppb when measuring alongside the plume (Panel 6) and much lower values when measuring orthogonally to it (e.g. Panel 3). A small NO_2 enhancement of 4×10^{15} molec/cm^2 is seen in the zenith sky measurements around 12:50 UTC, which is gone at 12:55 UTC, indicating that at least part of the plume was located above the MAX-DOAS instrument. As the zenith sky measurements are used as a sequential reference for the off-axis measurements, this causes a small canceling effect when using the sequential reference. As off-axis DSCDs are on the order of 1×10^{17} molec/cm^2 reaching up to 1.4×10^{17} molec/cm^2 as can be seen from Fig. 3, the overall impact on the path averaged VMRs is very small, on the order of 2 to 4 %.

Starting with Panel 9 the in situ ~~values are even higher , with more than 5 , which is~~ instrument measures even higher values, which are not represented in the figure as the color scale extending up to 5 ppb is saturated. ~~This is~~ In Panel 9 increasing to 6.1 ppb, in Panel 10 and 11 topping at 8.3 ppb and 8.9 ppb, respectively. In Panel 12 the measured NO_2 VMR drops to 6.3 ppb but increases again due to the second plume, reaching 6.6 ppb, 6.8 ppb and 7.1 ppb in Panels 13 to 15. After Panel 15, the value increases further to 8.8 ppb and goes down again to ambient background concentrations. This means that the in situ instrument measured two overlapping plumes. The maximum in situ NO_2 VMRs are much higher compared to the MAX-DOAS measurements, because the in situ instrument measures directly the NO_2 VMR inside the plume and the MAX-DOAS delivers ~~only~~ path-averaged values, which underestimate the local VMR inside the plume. The fact that the plume overpass is seen earlier in the MAX-DOAS zenith sky measurements than in the in situ measurements indicates that wind speeds are higher at higher altitudes, so that the upper part of the plume crossed the radar tower earlier than the lower part.

In Panel 11 the ship plume has moved out of the narrow line of sight of the MAX-DOAS instrument and measured NO_2 values drop rapidly to ambient concentrations on ~~all lightboth~~ both path segments. Panels 11 to 14 show all low MAX-DOAS measurements, while the plumes of both ships are hitting the radar tower leading to a very high in situ signal.

In Panel 15 the larger ship has moved further away from the instrument, leading for the first time in this sequence to a higher concentration on ΔL, far away from the instrument, than close by. Comparing the locations of the MAX-DOAS paths with the ship position and modeled plume in detail, however, indicates a much larger intersect of the plume with the UV path than with ΔL. This might be an example probably showing the uncertainty (overestimation) in the path length estimation due to negligence of the correction factor as discussed in Section 3.1.

Figure 5 shows again, but in more detail the measurements, ship and plume positions from Panel 10. To highlight the entire retrieved two dimensional NO_2 field in the measurement region along the shipping lane, the four previous MAX-DOAS measurements are shown as well, which were measured between 30 seconds and 3 minutes before. The strong horizontal

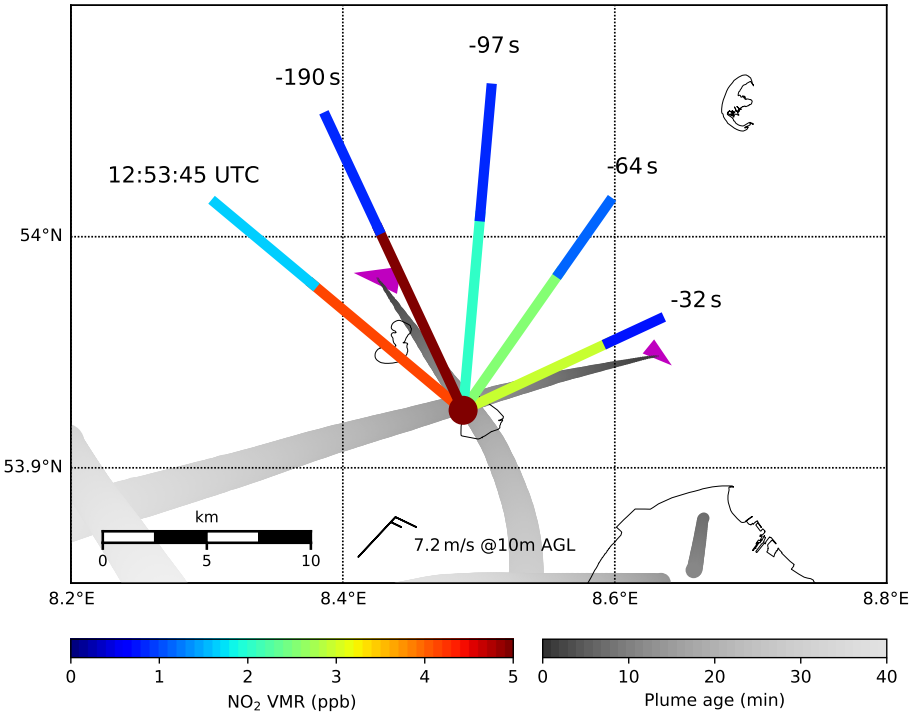

Figure 5. Map showing a zoom in onto Panel 10 of Figure 4 and the four previous MAX-DOAS ~~measurementsobservations~~observations, ~~being~~ which have been measured between 30 seconds and 3 minutes before the current observation. Horizontal light path lengths (UV path and ΔL) and corresponding path averaged volume mixing ratios of NO_2 are shown as colored lines, in situ NO_2 values as a colored dot at the location of the instrument. Magenta triangles show the ship position and course, with larger triangles for larger ships. ~~Gray stripes show forward trajectories~~ The modeled plumes are shown in gray, the lightness of the ~~emission plumes calculated from wind speed and direction for~~ gray shading representing the ~~moving ship~~plume age. Please keep in mind that ship and plume position were different for the past measurements. Wind direction and speed is shown with a meteorological wind barb.

gradient between enhanced NO_2 concentrations close to the site and low concentrations further away for such a north wind situation is clearly visible in the figure.

4.3 Southerly wind situations

The second selected case study shows a diametrically opposite situation: For southerly winds the emitted pollution plumes are blown to the north of the shipping lane (compare Fig. 1b), further away from the instruments. As a result, NO_2 concentrations south of the shipping lane, close to the instruments, should be low, resembling situation (b) in Fig. 2. On-site in situ instruments are not able to measure the ship emission plumes.

Figure ~~4~~ 6 shows a 12 minute sequence of consecutive measurements on 13 August 2014 starting at 12:35 UTC (14:35 local time). It shows MAX-DOAS path averaged NO_2 VMRs as well as ~~in-situ measurements.~~ in situ measurements. Shown are

also ship positions and course from AIS data, plume trajectories (see Section 3.3) and wind speed and direction measured by the weather station on Neuwerk.

In the map sequence, three ships can be seen on the shipping lane, two large ones (336 m and 365 m) and a smaller one (100 m). As all ships move in the same, eastward, direction, the plume trajectories are almost parallel. Apart from the ship emission plumes, another plume crosses the area of interest, originating from the two directly adjacent coal-fired power plants in Wilhelmshaven, located at 53.57°N, 8.14°E, in a distance of about 50 km, southwest of the measurement site. Using the 10 m a.g.l. wind speed of $7.5 \pm 1.0\,\mathrm{m\,s^{-1}}$ the plume age is estimated to be around 110 minutes, and even shorter taking into account that wind speed increases with height.

For the plume modeling, the stability class C representing slightly unstable conditions has been selected based on the wind speed and the strong solar insolation on this clear sky day.

Panel 1 shows the MAX-DOAS measurement at 12:35:31 UTC in the 310° azimuth direction. The horizontal path averaged NO_2 VMR along the UV light path is low (∼0.6 ppb) and on ΔL slightly enhanced (∼1 ppb), meaning low NO_2 close to the instrument and enhanced NO_2 further away (than the UV scattering point). The source for the enhanced NO_2 signal on ΔL could either be the small ship's plume or plumes from the more distant power plants.

The next measurement in Panel 2 at 335° azimuth gives similar results. In this viewing direction the plume of the small ship is not in the line of sight of the instrument, indicating that the plume originating from the power plants is the source of the slightly enhanced NO_2 VMR along ΔL.

In Panel 3 (5° azimuth) the MAX-DOAS instrument is measuring towards the two adjacent plumes of the two large ships, one located close to the UV scattering point and the other one further away. NO_2 VMR is high (∼2 ppb) behind the UV scattering point and medium high (∼1 ppb) closer to the instrument.

Panel 4 (35° azimuth) shows again high values far away from the instrument and medium high values close by.

In Panel 5 (65° azimuth), only one of the two plumes is in the line of sight and is further away than the UV scattering point, leading to enhanced NO_2 along ΔL and low (ambient) NO_2 along the UV path.

Panels 6 and 7 are similar to Panels 1 and 2, showing that the situation in these viewing direction has not changed four minutes later.

In Panel 8, four minutes after Panel 3, the plumes of the two big ships traveled a bit further northward, making the gradient between NO_2 VMRs on UV path and ΔL even stronger.

Panels 10 to 12 are similar to Panels 5 to 7.

In Panels 13 to 15, the plumes of the two big ships are now clearly only probed by the visible light path giving enhanced NO_2 concentrations along ΔL and low, ambient NO_2 concentrations along the UV path.

In all 15 consecutive measurements shown in the map sequence the in situ instrument measured constantly low values. This indicates that for southerly winds it cannot detect ship emission plumes at this site. Measured NO_2 VMRs agree very well with ambient NO_2 VMRs from the MAX-DOAS, retrieved south of the shipping lane along the UV path.

Figure 7 shows again in more detail the measurements, ship and plume positions from Panel 15. To highlight the entire retrieved two dimensional NO_2 field in the measurement region along the shipping lane, the four previous MAX-DOAS

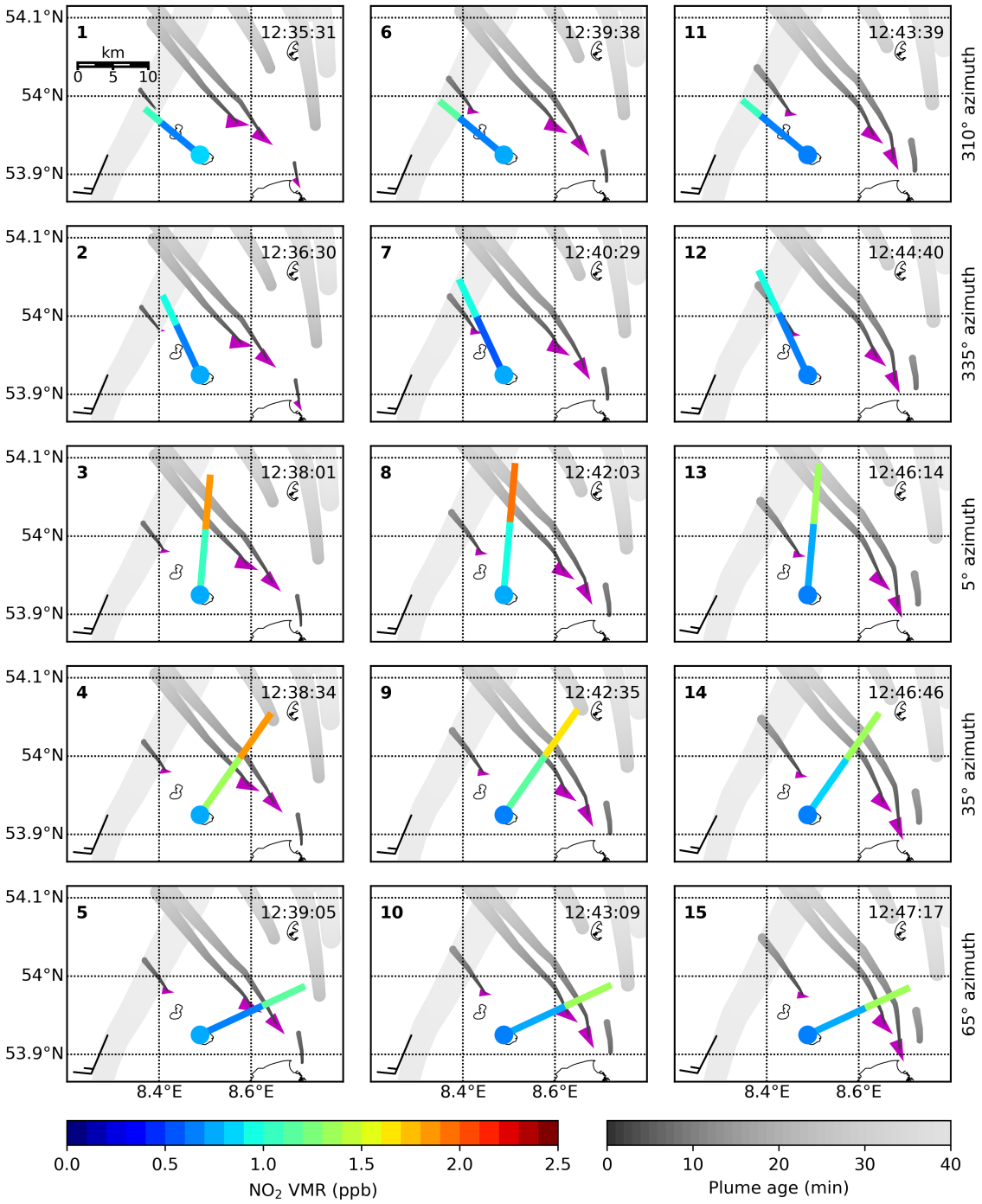

Figure 6. Sequence of maps showing 15 consecutive measurements in 0.5° elevation on 13 August 2014, starting at 12:35 UTC (14:35 local time): The extent of the UV path and ΔL and corresponding path averaged NO_2 VMRs are shown as colored lines. In situ NO_2 VMRs are shown as a colored dot at the location of the measurement site. Magenta triangles show the ship position and course (sharp tip), with larger triangles for larger ships. ~~Gray stripes show forward trajectories~~ The modeled plumes are shown in gray, the lightness of the ~~emission plumes calculated from wind speed and direction for~~ gray shading representing the ~~moving ship~~plume age. Wind direction and speed is shown with meteorological wind barbs.

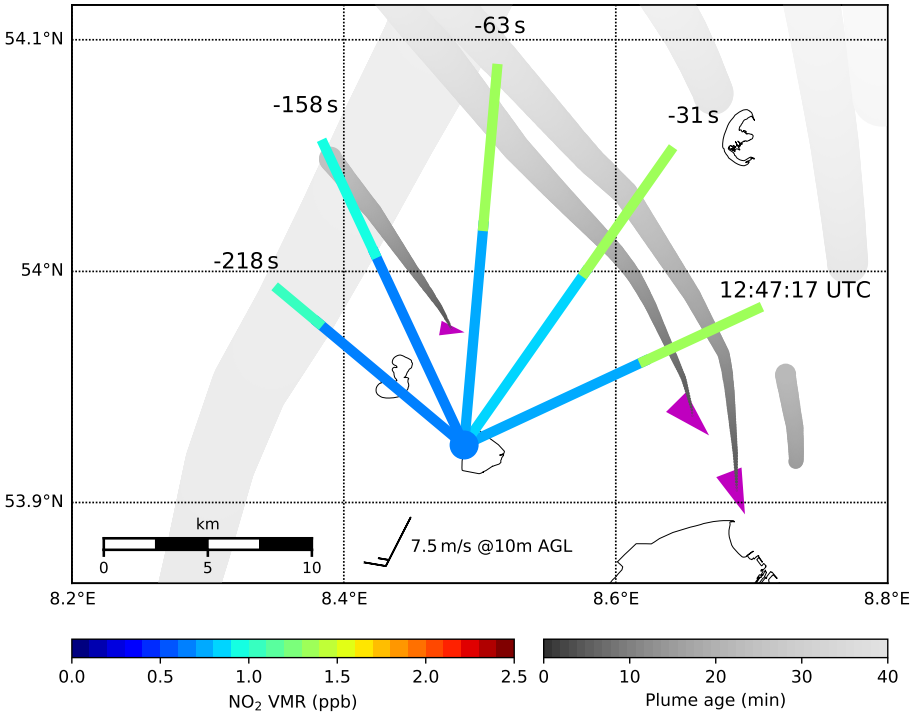

Figure 7. Map showing a zoom in onto Panel 15 of Figure 6 and also the four previous MAX-DOAS observations, ~~being~~ which have been measured between 30 seconds and 3.5 minutes before the current observation. Horizontal light path lengths and corresponding path averaged volume mixing ratios of NO_2 are shown as colored lines, in situ NO_2 values as a colored dot at the location of the instrument. Magenta triangles show the ship position and course, with larger triangles for larger ships. ~~Gray stripes show forward trajectories~~ The modeled plumes are shown in gray, the lightness of the ~~emission plumes calculated from wind speed and direction for~~ gray shading representing the ~~moving ship~~plume age. The broader plume in the eastern part of the map originates from the Wilhelmshaven power plants. Please keep in mind that ship and plume position were different for the past measurements. Wind direction and speed is shown with a meteorological wind barb.

measurements are shown as well, ~~being~~ which have been measured between 30 seconds and 3.5 minutes before. It highlights the horizontal gradient between low NO_2 concentrations close to the site and enhanced concentrations further away, northward of the shipping lane, demonstrating that with MAX-DOAS it is well feasible to measure ship emission plumes under conditions unfavorable for in situ measurements.

5 ~~Comparison of NO_2 VMRs retrieved from MAX-DOAS with airborne imaging DOAS measurements during the NOSE campaign 2013~~

4.1 Computation of in-plume NO_2 volume mixing ratios using plume modeling and validation with airborne imaging DOAS measurements

~~To validate the onion peeling~~ In addition to visualizing the two-dimensional NO_2 field over the shipping lane, plume modeling allows to retrieve in-plume NO_2 VMRs from the MAX-DOAS ~~approach, the~~ measurements. For a demonstration of the method, a day was chosen on which simultaneous airborne imaging DOAS measurements were performed, which can be used to validate both the plume modeling and the MAX-DOAS in-plume NO_2 VMRs.

4.1.1 Computation of in-plume NO_2 VMRs

The O_4 scaling and onion peeling method yields NO_2 VMRs which are averaged along a certain effective horizontal light path. In the general case that the plume does not cover the entire path, the retrieved path-averaged VMR is lower than the in-plume VMR. Thus, to retrieve the in-plume VMR, the fraction of the path probing the plume and thus the plume width has to be known. An estimate for the plume width is provided by the combination of forward trajectory and Gaussian plume model implemented in this study.

Figure 8 shows MAX-DOAS path averaged NO_2 VMRs and modeled plumes on 21 August 2013 around 9:53 UTC (11:53 local time). Also shown are AirMAP vertical columns of NO_2 ~~VMRs retrieved from the~~ which are used for validation in the second part of this section (see Section 4.1.2 for more details).

The Gaussian plume model was run for a stability class of B–C, which was selected due to the moderate insolation (cloudy in the morning, later clearing up) and wind speeds between 3 and 4 meters per second. For this intermediate stability class B–C, representing slightly to moderately unstable conditions, the mean of the parameter values for B and C from Tab. 3 is taken. Wind speed and direction are taken from the weather station on Scharhörn.

Along ΔL where one of the modeled plumes is located, he MAX-DOAS ~~measurements have been compared to other, independent measurements.~~ measured enhanced NO_2 compared to the ambient background NO_2 measured along the UV path. This plume originates, the one from the 277 m ship that left the map region to the west. At the intersection of plume and MAX-DOAS line-of-sight, the plume air parcels had traveled a distance of (2180 ± 30) m in (660 ± 10) s since emission and the plume model yields a width of (720 ± 20) m. The selection of the stability class clearly has a strong influence on the modeled plume width, as the more unstable class B yields (870 ± 20) m and the more stable class C yields (580 ± 20) m. This span of values gives a more realistic error estimate. The MAX-DOAS LOS "hits" the plume at an angle of approximately 70°, so the resulting effective plume width is (760 ± 160) m.

For the computation of the MAX-DOAS average in-plume NO_2 VMR, the partial horizontal column inside the plume has to be determined as only scaling the VMR would not account for the background signal. The three panels in Fig. 9 show the MAX-DOAS DSCDs of NO_2 for the lowest 5 elevation angles measured in the UV and visible spectral range, as well as their differences, ΔDSCD.

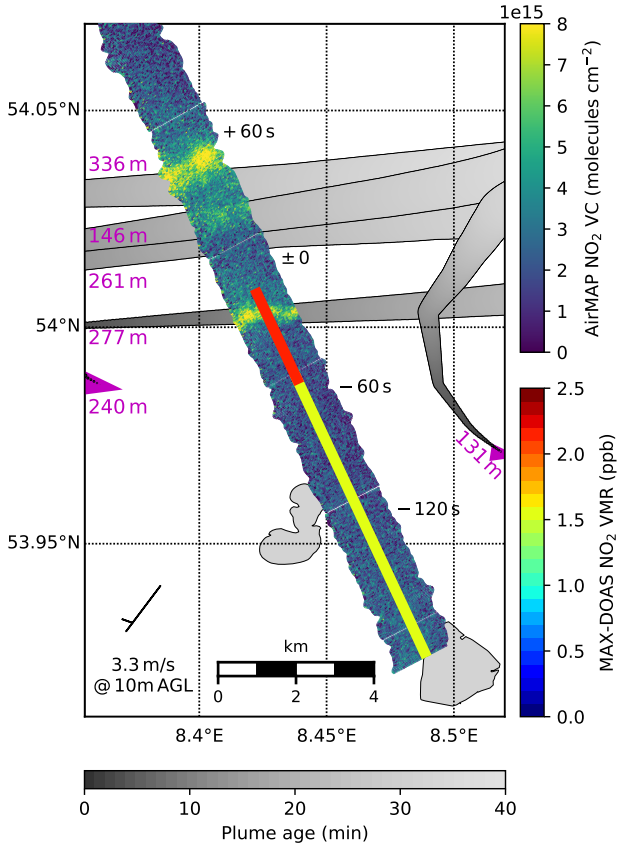

Figure 8. Map showing the MAX-DOAS path averaged VMRs (colored lines) and AirMAP vertical columns of NO_2 (broad image stripe beneath) on 21 August 2013 around 9:53 UTC (11:53 local time). As the plotted physical quantities are entirely different (VMRs and columns), color scale agreements are not expected (and completely random). Magenta triangles show current ship positions and course, magenta numbers denote the ship length. The modeled plumes (for the MAX-DOAS measurement time) are shown in gray, the lightness of the gray shading representing the plume age. The time difference between AirMAP and MAX-DOAS measurements is indicated in the map at specific parts of the flight track. Wind direction and speed is shown with a meteorological wind barb.

At 9:53 UTC a ΔDSDC of $1.3 \times 10^{16}\,\mathrm{molec\,cm^{-2}}$ is measured along a 2.4km ΔL. The UV measurement of $3.0 \times 10^{16}\,\mathrm{molec\,cm^{-2}}$ along a 7.7km L_{UV} can be used to estimate the background signal along ΔL. With the modeled plume width $b = (760 \pm 160)\,\mathrm{m} = (76000 \pm$ this yields for the column inside the plume:

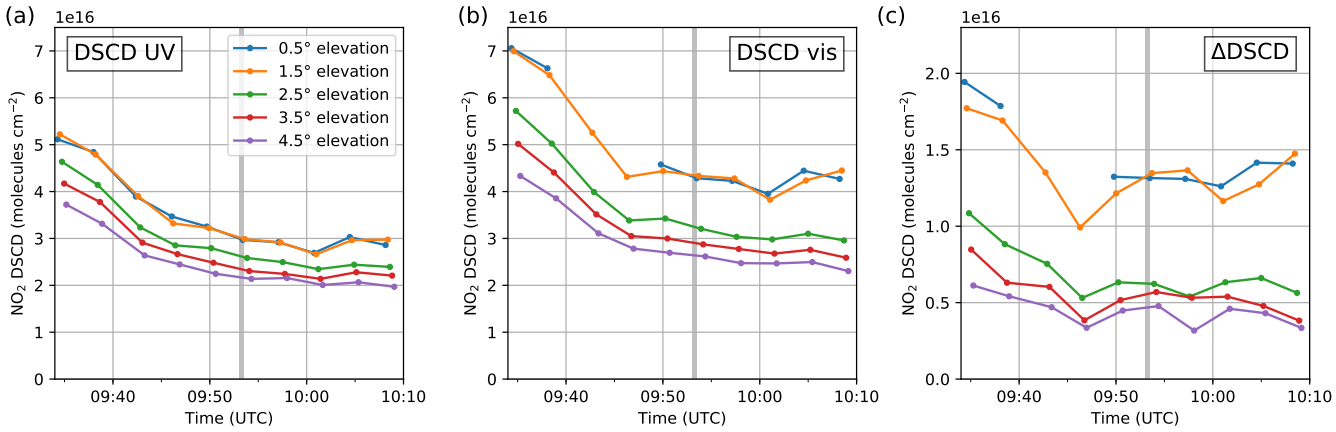

Figure 9. MAX-DOAS differential slant column densities of NO_2 in the UV (a) and visible (b) spectral range as well as their difference ΔDSDC (c) for the five lowest elevation angles for the azimuthal viewing direction of 335°. The vertical gray line indicates the AirMAP plume overpass time.

$$\begin{aligned}\mathrm{DSCD_{plume}} &= \Delta\mathrm{DSCD} - \mathrm{DSCD_{background}} \\ &= \Delta\mathrm{DSCD} - \mathrm{DSCD_{UV}} \cdot \frac{\Delta L - b}{L_{\mathrm{UV}}} \\ &= (6.9 \pm 3.1) \times 10^{15}\,\mathrm{molec\,cm^{-2}}\end{aligned}$$

where the associated uncertainty has been computed with Gaussian error propagation from the uncertainties of the retrieved DSCDs (±10 %), path lengths (±20 %) and modeled plume width (see above) assuming independent random uncertainties in the individual variables.

The average VMR inside the plume is given by:

$$\mathrm{VMR_{plume}} = \frac{\mathrm{DSCD_{plume}}}{b \cdot n_{\mathrm{air}}} = (3.6 \pm 1.8) \times 10^{-9} = (3.6 \pm 1.8)\,\mathrm{ppb}$$

where $n_{\mathrm{air}} = 2.54 \times 10^{19}\,\mathrm{molec\,cm^{-3}}$ is the number density of air for the measured pressure of 1025.2 hPa and temperature of 19.2 °C. The total uncertainty has again been computed with error propagation.

4.1.2 Validation

As already indicated above, ~~the~~ a comparison to on-site in situ trace gas analyzers is well suited ~~for~~ to validate the MAX-DOAS ambient NO_2 background values~~or specific constellations~~, but fails for in-plume concentrations in many constellations. For

unfavorable wind conditions, like southerly winds, the in situ instrument does not detect the plumes at all. The spatial resolution of satellite instruments is not sufficient to resolve individual ship plumes, even with the ~~newest~~ Sentinel 5 precursor satellite ($3.5 \times 7\,\mathrm{km}^2$, Veefkind et al. 2012).

Airborne imaging DOAS measurements~~are the ideal method to compare to, at least on a campaign base, since they can deliver high resolution NO_2 maps along the azimuthal viewing directions of the instrument. Such measurement~~ , as have been performed in the region of interest during the NOSE (for german "Nord-Ost-See-Experiment" meaning "North and Baltic sea experiment") campaign (Meier, 2018) on 21 August ~~2013.~~ 2013, are the ideal method for validation of our results. Mapping of the MAX-DOAS line-of-sights, as has been done during NOSE, allows to compare the approximate plume position retrieved from the onion peeling MAX-DOAS method and those from the plume modeling to the real plume position.

4.2 ~~AirMAP instrument and data analysis~~

Delivering high resolution NO_2 maps of the plumes, the airborne measurements can be used to validate both the plume positions calculated with simple forward trajectories and the plume width retrieved from the Gaussian plume model. By incorporating plume height information from either plume modeling or the vertical elevation scans of the MAX-DOAS, an average in-plume NO_2 VMR can be computed from the airborne vertical column measurements and compared to the result from the MAX-DOAS.

The ~~Airborne imaging Differential Optical Absorption Spectroscopy instrument for Measurements of Atmospheric Pollution~~ *Airborne imaging Differential Optical Absorption Spectroscopy instrument for Measurements of Atmospheric Pollution* (AirMAP), being installed on a Cessna research aircraft of the Freie Universität Berlin for the measurements, is a push-broom imaging DOAS instrument. Scattered sunlight from below the aircraft is collected by a wide-angle objective and coupled into a ~~sorted~~ bundle of 35 sorted optical fibers. The image of the vertically stacked fibers is then dispersed by an imaging grating spectrometer and mapped onto a frame-transfer-CCD. The total field of view of around 52° leads to a ground swath width similar to the flight altitude. With this set-up, 35 across track pixels are measured simultaneously with an exposure time of 0.5 seconds, leading to a spatial resolution better than 50 m when the aircraft is flying at 1600 m altitude. For more detailed information on the instrument see Schönhardt et al. (2015) and Meier et al. (2017).

~~Differential~~ In the AirMAP data analysis, differential slant column densities of NO_2 were retrieved in a fit window of 425-450 nm using the settings described in Meier et al. (2017). For the retrieval of NO_2 vertical column densities, air mass factors were calculated for an NO_2 box profile assuming constant NO_2 in the lowest 500 ~~m~~m, in an atmosphere without aerosols and for a constant surface reflectance of 0.05.

4.2 ~~NOSE campaign 2013~~

~~The NOSE campaign took place in northern Germany in August 2013 aiming at the measurement of shipping emissions in support of the MESMART project. On 21 August between 9:00 and 12:30 UTC a flight over the Neuwerk region was performed with a flight pattern covering the individual MAX-DOAS azimuthal viewing directions. In addition to that, a low level flight~~

over an individual ship following the emitted plume was performed. For more detailed information on the NOSE campaign see Meier (2018).

4.2 Comparison between MAX-DOAS and AirMAP

The combination of ground-based MAX-DOAS with airborne imaging DOAS measurements provides mutual benefits for the interpretation of the measurements: The combination of both methods makes it possible to derive in-plume NO_2 concentrations from each method.

The onion peeling MAX-DOAS approach delivers horizontal path averaged concentrations. As discussed in Section 3.1, ship emission plumesusually fill only a small fraction of these light path segments. The average over the path segment will therefore strongly underestimate the concentration inside the plume. To retrieve the in-plume concentration, the horizontal plume extent has to be known. AirMAP high resolution NO_2 maps can provide this information.

The AirMAP measurements deliver vertical columns of NO_2 between ground and aircraft, but no information about the vertical location of the NO_2 inside the column. By assuming a box profile for the near-ground NO_2 layer, one can derive concentrations from the vertical columns. The MAX-DOAS vertical scan can provide an estimation for the vertical extent of the plumeThis box profile height is an educated guess on an upper limit for the typical vertical plume extent for older ship plumes, which the plume modeling has proven to be in the right order of magnitude.

The crucial differences in viewing geometries are sketched in Fig. 10. The MAX-DOAS instrument scans the plume vertically by using different elevation angles giving (slanted) horizontal transects of the plume. The AirMAP instrument, measuring in nadir direction downward from the aircraft, observes vertical transects of the plume. The plume height h can be roughly estimated from the MAX-DOAS measurements if the distance is known, while the plume position and width b can be obtained from the airborne observations. Hence, the combination of both observation geometries can be used to narrow down the plume's extent in space.

Sketch of the different measurement geometries of ground-based MAX-DOAS and airborne imaging DOAS instrument when measuring a ship plume. While the MAX-DOAS instrument scans the plume vertically, the AirMAP instrument measures in nadir direction. Distances and sizes are not up to scale.

Figure 8 shows Fig. 8, already mentioned in the previous subsection, shows additionally to the MAX-DOAS path averaged VMRs along with the AirMAP vertical columns of NO_2 for a ship plume measured on 21 August 2013 around 9:53 UTC (11:53 local time). The Cessna airplane, a research aircraft of the Freie Universität Berlin, housing the AirMAP instrument At about that time, the aircraft flew along the MAX-DOAS 335° azimuth line of sight of the instrument line-of-sight crossing the shipping lane and mapping multiple ship plumes. Enhanced NO_2 is measured where the aircraft overpasses the emission overpassed the plumes, revealing the location and horizontal extent of the plumes. The southernmost plume was also covered by the MAX-DOAS instrument's NO_2 measurement in the visible spectral range. As a result, the path averaged NO_2 VMR along ΔL shows enhanced values compared to the ambient background NO_2 measured along the UV path., indicating a plume somewhere along ΔL, which is validated by the airborne measurements. Along the UV path AirMAP NO_2 VCDs are significantly lower confirming the assumption of ambient background pollution.

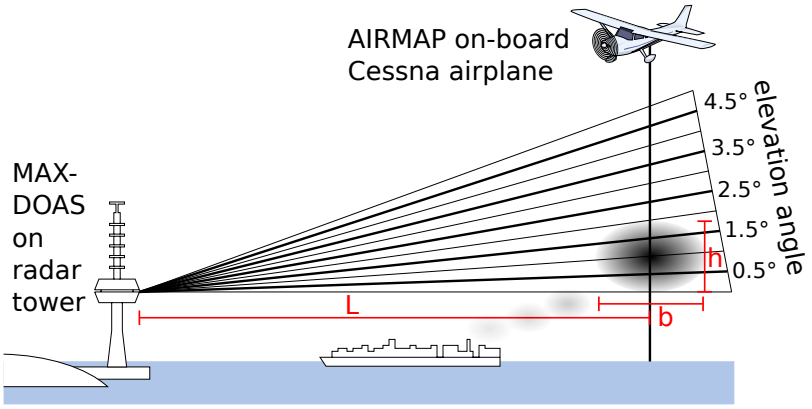

Figure 10. ~~Map showing the MAX-DOAS path averaged VMRs (colored lines) and AirMAP vertical columns~~ Sketch of ~~NO_2 (broad image stripe beneath) on 21 August 2013 around 9:53 UTC (11:53 local time). As~~ the ~~plotted physical quantities are entirely~~ different ~~(VMRs and columns), color scale agreements are not expected~~ (measurement geometries of ground-based MAX-DOAS and ~~completely random). Magenta triangles show current~~ airborne imaging DOAS instrument when measuring a ship ~~positions and course~~plume. ~~Grey stripes show forward trajectories of the ship emission plumes calculated from wind speed and direction for~~ While the MAX-DOAS ~~measurement time. The time difference between AirMAP and MAX-DOAS measurements is indicated in~~ instrument scans the ~~map at specific parts of~~ plume vertically, the ~~flight track. Wind~~ AirMAP instrument measures in nadir direction. Distances, heights and ~~speed is shown with a meteorological wind barb~~sizes are not to scale.

The time difference between both measurements of less than 20 seconds is very small~~as stated in the map~~, especially considering the integration time of the MAX-DOAS instrument of 10 seconds. The ~~calculated forward trajectory of this plume matches the AirMAP measurements~~position of the plume (calculated with a forward trajectory) and the horizontal extent of the plume (computed with the Gaussian plume model) matches the real plume positions measured by AirMAP very well. The plumes further north have been measured by AirMAP around 1 minute later, enough time for the wind to blow the plumes northward so that the positions do not fully coincide with the plume forward trajectories which have been ~~calculated~~ computed for the MAX-DOAS measurement time.

~~The calculated plume trajectory matches~~ Inspecting the AirMAP measurements ~~very well (even better in the second example in Fig. 12) and the plume position derived from the onion peeling MAX-DOAS fits to the AirMAP measurements~~in detail reveals that the real plumes are not as smooth as the modeled plumes and show some irregularities and random fluctuations caused by turbulence. This deviation is expected, as the Gaussian plume model used here assumes a steady state and describes a (long) time averaged picture of a plume. Nevertheless, the modeled plume widths fit quite well. These results provide confidence in the ~~calculated~~ modeled plume trajectories, as well as in the onion peeling approach to detect locally enhanced NO_2 levels in the ΔL light path segment.

~~Figure 11a shows NO_2 VCDs from AirMAP as a function of distance to the radar tower for the flight track section shown~~ For the validation of the in-plume NO_2 VMR by AirMAP, one has to consider the crucial differences in viewing geometries

which are sketched in Fig. ~~8. The 35 individual viewing directions were binned to 5 (1:7, 8:14, 15:21, 22:28 and 29:35) to reduce the noise. Although additional binning would reduce the noise even further, it would also smear out the plume signal, since the flight track crosses the plumenot orthogonally but at an angle of about 70°(see Fig. 8). A strong enhancement~~ 10. The MAX-DOAS instrument measures (slightly slanted) horizontal transects of the plume and can scan the plume vertically by using different elevation angles. The AirMAP instrument, measuring in nadir direction downward from the aircraft, observes vertical transects of the plume. The AirMAP measurements deliver vertical columns of NO_2 ~~is observed at a distance of about 9.1 km to 10.1 km. This interval is covered by the visible light path but not the UV path, which means it is completely inside the path difference ΔL. Along the UV path NO_2 VCDs are significantly lower representing ambient background pollution. There is a slight decrease of ambient~~ between ground and aircraft, but no information about the vertical location of the NO_2 inside the column. By assuming a box profile for the near-ground NO_2 ~~observed along the UV path from the radar tower towards the UV scattering point. Figure 11b shows the measurements of the plume in more detail, revealing the distance shift~~ layer (the plume), one can derive mixing ratios from the vertical columns, but for this the vertical extent of the plume ~~position in the different viewing directions due to the slanted angle between flight direction and plume . The NO_2 enhancement caused by~~ has to be known. This plume height h can either be taken from the plume modeling or can roughly be estimated from the MAX-DOAS vertical scan measurements if the distance to the plume is ~~roughly Gaussian-shaped in all 5 binned viewing directions, although maximum values and peak widths differ sligthly~~known, as it is from the airborne measurements.

~~AirMAP vertical columns of NO_2 as a function of distance (lower axis) or time (upper axis) for the flight track section shown in Fig. 8. The right plot is a zoom in on the grey shaded area. Horizontal arrows denote the horizontal effective light paths.~~

~~The measured vertical columns are total columns between flight altitude and ground level. To retrieve the local enhancement of NO_2 inside the plume,~~ The Gaussian plume model delivers a height of (320 ± 20) m reaching from the ground to this height at the respective distance from the emission point (see above) for the selected stability class B–C and for a stack height of 40 m estimated from pictures of the ship and an assumed initial plume rise of 10 m. Again, the selection of the ~~background (ambient)column is subtracted from the total NO_2 column:~~

$$\begin{aligned} \mathrm{VC_{plume}} &= \mathrm{VC_{total}} - \mathrm{VC_{background}} \\ &= (7 \pm 1) \times 10^{15}\,\mathrm{molec\,cm^{-2}} - (2.0 \pm 0.2) \times 10^{15}\,\mathrm{molec\,cm^{-2}} \\ &= (5 \pm 1) \times 10^{15}\,\mathrm{molec\,cm^{-2}} \end{aligned}$$

stability class has an influence on the modeled plume height, with (420 ± 20) m retrieved for the more unstable class B and (230 ± 20) m for the more stable class C, the span giving again an idea on the uncertainty introduced by the selection of the stability class.

~~The plume width b can be estimated from the measurements as $b = 500\,\mathrm{m} \pm 100\,\mathrm{m}$.The three panels in Figure 9show~~ For the estimation from the MAX-DOAS measurements, we need to reconsider Fig. 9, showing the MAX-DOAS DSCDs of NO_2 for ~~the lowest 5 elevation angles measured in the~~ UV and visible spectral range ~~,~~ as well as ~~their difference,~~ the ΔDSCD. The UV measurements in Panel (a) show the typical elevation angle dependency for tropospheric absorbers, with longest light paths

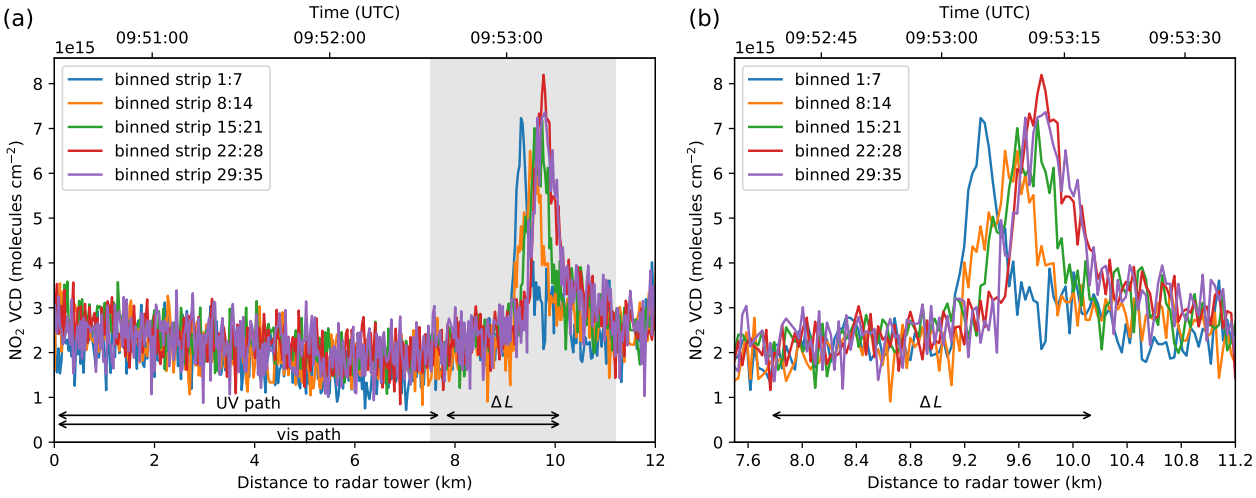

Figure 11. AirMAP vertical columns of NO_2 as a function of distance (lower axis) or time (upper axis) for the flight track section shown in Fig. 8. The right plot is a zoom in on the gray shaded area. Horizontal arrows denote the horizontal effective light paths.

~~(~~and therefore highest DSCDs ~~)~~ in the lowest elevation angles. When the instrument points further up (i.e. higher elevation angles), the light path ~~lengths~~ length through the troposphere ~~decrease~~ decreases giving smaller DSCDs.

~~MAX-DOAS differential slant column densities of NO_2 in the UV (a) and visible (b) spectral range as well as their difference ΔDSDC (c) for the five lowest elevation angles for the azimuthal viewing direction of 335°. The vertical gray line indicates the AirMAP plume overpass time.~~

Comparing Panel (b), showing the visible measurements, to Panel (a), the values are in general larger due to the longer light path length for longer wavelengths but show a similar separation except for the "gap" between the low elevations (0.5°, 1.5°) and higher elevations (2.5°, 3.5°, 4.5°). This implies that there is even more additional NO_2 in the lower elevations than is expected from the longer light path ~~lengths in the visible~~effect. The gap is even more pronounced when ~~calculating the differences between both DSCDs,~~ inspecting the ΔDSCD shown in Panel (c). ~~The~~ This excess NO_2 most certainly originates from the ship emission plume. Assuming that the plume vertically fills the whole vertical field of view of the 0.5° and 1.5° elevation an upper boundary for the plume height h can be calculated. The field of view of the instrument is around 1.0°. Thus the plume is observed in a solid angle of 2.0° (~~see~~ compare Fig. 10). At a distance of 9.6 ~~km~~km (see below), this corresponds to a plume height of $h = 9.6\,\mathrm{km}\cdot\tan 2° \approx 335\,\mathrm{m}$. This result is in good agreement with the plume modeling result of (320 ± 90) m.

~~The plume , as can be seen~~

Figure 11a shows NO_2 VCDs from AirMAP as a function of distance to the radar tower for the flight track section shown in Fig. 8~~and 11b, is only partly covered by the ΔL light path segment. To retrieve the in-plume NO_2 DSCD, the ambient~~. The 35 individual viewing directions were binned to 5 (1:7, 8:14, 15:21, 22:28 and 29:35) to reduce the noise. Although

additional binning would reduce the noise even further, it would also smear out the plume signal, since the flight track crosses the plume not orthogonally but at an angle of about 70° (see Fig. 8). A strong enhancement of NO_2 ~~background within~~ is observed at a distance of about 9.1 km to 10.1 km, as it was expected from the MAX-DOAS NO_2 enhancement along ΔL ~~has to be subtracted. This can either be estimated from the measurements in the slightly higher elevations, which presumably do not contain plume NO_2, assuming constant~~ . Figure 11b shows the measurements of the plume in more detail, revealing the distance shift of the plume position in the different AirMAP viewing directions due to the slanted angle between flight direction and plume. The NO_2 ~~background in the lower altitudes, or from the column along the UV light path. This is not trivial, since the ambient~~ enhancement caused by the plume is roughly Gaussian-shaped in all 5 binned viewing directions, confirming that the Gaussian plume model gives a good approximation of the plume shape, although maximum values and peak widths differ due to the turbulent fluctuations.

The measured vertical columns are total columns between flight altitude and ground level. To retrieve the local enhancement of NO_2 ~~is not constant along this path, but increases towards the radar tower, as can be seen in Fig. 11a. Whether this slightly enhanced~~ inside the plume, the estimated background column containing ambient NO_2 is subtracted from the total NO_2 ~~is in the right height to be probed by the instruments field of view, is unknown. Either way, both estimations end up with a similar background column of $(6 \pm 1) \times 10^{15}$ molec cm^{-2}, the error margin reflecting the underlying uncertainty . This yields:~~ column:

$$\begin{aligned} \mathrm{VC}_{\mathrm{plume}} &= \mathrm{VC}_{\mathrm{total}} - \mathrm{VC}_{\mathrm{background}} \\ &= (7.0 \pm 2.0) \times 10^{15}\,\mathrm{molec\,cm^{-2}} - (3.2 \pm 1.0) \times 10^{15}\,\mathrm{molec\,cm^{-2}} \\ &= (3.8 \pm 2.2) \times 10^{15}\,\mathrm{molec\,cm^{-2}} \end{aligned}$$

$$\begin{aligned} \mathrm{DSCD}_{\mathrm{plume}} &= \Delta\mathrm{DSCD} - \mathrm{DSCD}_{\mathrm{background}} \\ &\approx (13.3 \pm 0.2) \times 10^{15}\,\mathrm{molec\,cm^{-2}} - (6 \pm 1) \times 10^{15}\,\mathrm{molec\,cm^{-2}} \\ &= (7 \pm 1) \times 10^{15}\,\mathrm{molec\,cm^{-2}} \end{aligned}$$

Possible error sources for the AirMAP measurements are fitting uncertainties on the retrieved DSCDs, uncertainties on the surface reflectance, the assumed profile shape and aerosols, while uncertainties on the NO_2 amount in the reference spectrum cancel out when subtracting the background, yielding a maximum overall uncertainty on the NO_2 VCD of about 30 % (Meier et al., 2017).

The NO_2 columns measured horizontally (MAX-DOAS) and vertically (AirMAP) through the plume are different. This is expected, because the horizontal and vertical extent of the plume differ – the plume width ~~is~~ being approximately two times larger than its height. For a quantitative comparison, the in-plume NO_2 column ~~densities of both measurements need~~ density needs to be converted to ~~VMRs. With the plume height derived from~~ an average in-plume VMR.

$$\mathrm{VMR_{plume}} = \frac{\mathrm{VC_{plume}}}{h \cdot n_{\mathrm{air}}}$$

yielding (4.7 ± 3.0) ppb for $h = 320$ m (from plume model) or (4.5 ± 2.7) ppb for $h = 335$ m (from MAX-DOAS ~~measurements~~), where the overall uncertainty has been computed with error propagation.

This result is in reasonably good agreement with the average in-plume VMR of (3.6 ± 1.8) ppb derived from the ~~NO_2 VMR inside the plume can be calculated for~~ MAX-DOAS measurements combined with the Gaussian plume model. Having the AirMAP measurements for validation, the plume width computed by the plume model can be compared to the AirMAP measurements ~~:~~

$$\mathrm{VMR_{plume}} = \frac{\mathrm{VC_{plume}}}{h \cdot n_{\mathrm{air}}} \approx \frac{(5 \pm 1) \times 10^{15}\,\mathrm{molec\,cm^{-2}}}{33500\,\mathrm{cm} \cdot 2.54 \times 10^{19}\,\mathrm{molec\,cm^{-3}}}$$
$$= (6 \pm 1) \times 10^{-9} = (6 \pm 1)\,\mathrm{ppb}$$

~~where n_{air} is the number density of air for the measured pressure of 1025.2 and temperature of 19.2~~(Fig. 11). Using the same threshold as for the modeling, 1/e, this gives a plume width b of 600–700 ~~.~~

~~The horizontal extent of the plume derived~~ m, or an effective plume width of $b_{\mathrm{eff}} = (690 \pm 53)$ m due to the 70° angle between plume and flight direction. These values are in good agreement with the slightly higher values of $b = (720 \pm 150)$ m and $b_{\mathrm{eff}} = (760 \pm 160)$ m, respectively, computed by the model, again confirming the validity of the Gaussian plume modeling approach for this study. Using the more accurate plume width estimate from the AirMAP measurements ~~makes it possible to derive the same from~~, the MAX-DOAS ~~measurements:~~

$$\mathrm{VMR_{plume}} = \frac{\mathrm{DSCD_{plume}}}{b \cdot n_{\mathrm{air}}} \approx \frac{(7 \pm 1) \times 10^{15}\,\mathrm{molec\,cm^{-2}}}{50000\,\mathrm{cm} \cdot 2.54 \times 10^{19}\,\mathrm{molec\,cm^{-3}}}$$
$$= (5.5 \pm 0.8) \times 10^{-9} = (5.5 \pm 0.8)\,\mathrm{ppb}$$

~~These~~ in-plume VMR changes to a value of (4.0 ± 1.8) ppb giving an even better agreement with the AirMAP results. A thorough inspection of the AirMAP measurements along the UV path of the MAX-DOAS (see Fig. 8) reveals that there is a slight decrease of ambient NO_2 ~~VMRs retrieved from~~ background pollution observed along the UV path from the radar tower towards the UV scattering point and towards the plume location. Estimating the background column along ΔL from the UV path, where the MAX-DOAS ~~and AirMAP measurements agree well within their error margins~~delivers only one averaged value, thus might lead to a small bias in the background correction. If too much NO_2 is subtracted, the MAX-DOAS in-plume DSCD and VMR might be underestimated, which could explain the lower MAX-DOAS value compared to the AirMAP result.

~~Map showing the MAX-DOAS path averaged VMRs (colored lines) and AirMAP vertical columns of NO_2 (broad image stripe beneath) on 21 August 2013 around 9:43 UTC (11:43 local time). As the plotted physical quantities are entirely different (VMRs and columns), color scale agreements are not expected (and completely random). Magenta triangles show current ship positions and course. Grey stripes show forward trajectories of the ship emission plumes calculated from wind speed and direction for the MAX-DOAS measurement time. The time difference between AirMAP and MAX-DOAS measurements is~~

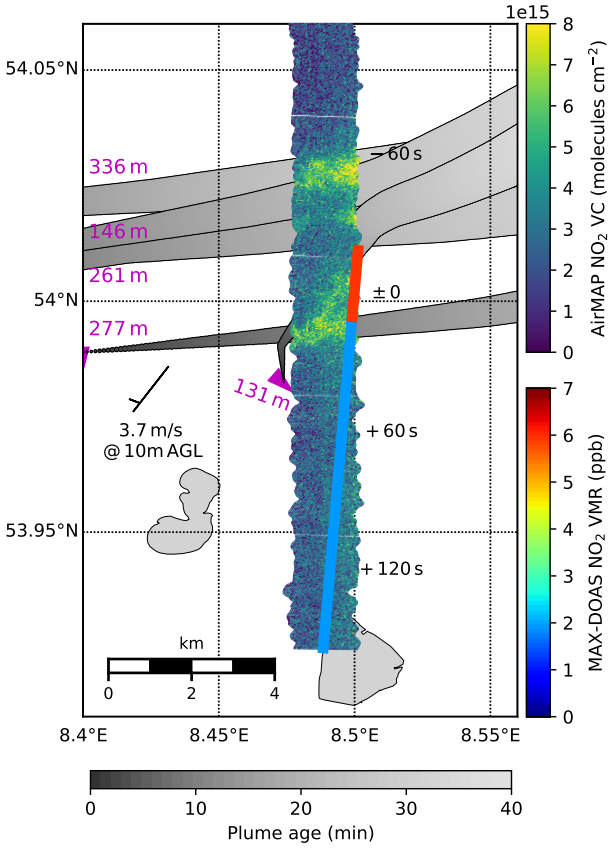

Figure 12. Map showing the MAX-DOAS path averaged VMRs (colored lines) and AirMAP vertical columns of NO_2 (broad image stripe beneath) on 21 August 2013 around 9:43 UTC (11:43 local time). Magenta triangles show current ship positions and course, magenta numbers denote the ship length. The modeled plumes (for the MAX-DOAS measurement time) are shown in gray, the lightness of the gray shading representing the plume age. The time difference between AirMAP and MAX-DOAS measurements is indicated in the map at specific parts of the flight track. Wind direction and speed is shown with a meteorological wind barb.

~~indicated in the map at specific parts of the flight track. Wind direction and speed is shown with a meteorological wind barb.~~ Another possible explanation for the lower MAX-DOAS values could be the underestimation of the VMR due to overestimation of path lengths because of negligence of correction factors as mentioned in Section 3.1.

Figure 12 presents another AirMAP overpass over several plumes from ten minutes earlier, again showing good agreement between the measured plume position and the approximate plume positions derived from the onion peeling MAX-DOAS. It shows even better how ~~projected plume trajectories~~ modeled plumes and real plume positions ~~derived from~~ measured by AirMAP fit together. A computation of in-plume VMRs is not possible in this case, as two plumes are located along ΔL and they are also not fully covered by ΔL.

5 Conclusions

The present study describes a novel application of the "onion-peeling" MAX-DOAS approach to measurements of shipping emissions to estimate the two-dimensional pollutant distribution in the strongly inhomogeneous NO_2 field over a shipping lane. The ability to probe air masses at different horizontal distances to the instrument to derive the approximate ship plume positions in the measurement area is shown on the basis of selected case studies out of the three year measurement period on the island Neuwerk. Located in the German Bight, 6–7 km south of the main shipping lane from the North sea into the river Elbe~~towards the harbor of Hamburg~~, the island was selected as an ideal site for the ~~application of the onion peeling approach. It is located~~ onion peeling MAX-DOAS approach as it is in a suitable distance to the shipping lane for exploiting the use of UV and visible radiation to probe the emission plumes released from the passing ships.

To determine the horizontal light path lengths for the onion peeling, a simple approach using the trace gas column of the oxygen collision complex, O_4 has been applied. To compare the measurements on the shorter UV path with the measurements on the longer visible path, ~~horizontal~~ path-averaged volume mixing ratios have been derived from the measured column amounts of NO_2. ~~In addition to that, the~~ For the "onion peeling", a separate NO_2 ~~mixing ratio on~~ VMR along the path difference, ~~which was~~ usually located over or close to the shipping lane ~~in our measurements, can be calculated~~ several kilometers away from the instrument, has been computed from UV and visible measurements, ~~providing the NO_2 concentration~~ allowing to compare NO_2 values close to the instrument (along the UV path) and several kilometers away ~~from the instrument~~(along the path difference).

~~For~~ It is shown that for northerly wind directions, the onion peeling MAX-DOAS can detect enhanced NO_2 concentrations close to the instrument south of the shipping lane and low NO_2 concentrations north of the shipping lane. For southerly wind directions, low NO_2 values are measured close to the site south of the shipping lane and enhanced NO_2 values in the north of the shipping lane, demonstrating that the MAX-DOAS instrument can detect pollution several kilometers away from the instrument under wind directions unfavorable for in situ measurements.

A ~~comparison to~~ combination of simple forward trajectories and a Gaussian plume model has been implemented to model the ship plumes, allowing to compute in-plume NO_2 volume mixing ratios from the MAX-DOAS measurements, which is demonstrated examplarily for a plume measured on 21 August 2013.

For validation of both the plume modeling and the MAX-DOAS results, airborne imaging DOAS measurements taken by the AirMAP instrument during the NOSE campaign ~~2013 shows the validity of the approach. The good agreement of AirMAPmeasured and~~ on this very same day have been used. AirMAP's measured plume positions agree well with the ones estimated by using the onion peeling MAX-DOAS ~~derived plume positions shows~~ approach showing that MAX-DOAS measurements can be used to derive the approximate position of ~~the~~ ship emission plumes. The good agreement of ~~plume locations calculated from wind and AIS data with the~~ modeled plume positions and shapes with AirMAP measurements shows that simple forward trajectories combined with a Gaussian plume model look-up-table approach provide sufficient accuracy to model the two-dimensional NO_2 field over the shipping lane. ~~Combining airborne vertical column and ground based horizontal column measurementsprovides mutual benefits, enabling the independent derivation of~~

By incorporating information about the vertical plume extent from either plume model or MAX-DOAS vertical scan measurements, an in-plume ~~volume mixing ratios from both measurement techniques~~NO_2 VMR has been derived from AirMAP measurements, too. AirMAP and MAX-DOAS in-plume ~~VMR~~ VMRs agree well within their error margins, ~~again~~ confirming the validity of the onion peeling MAX-DOAS approach and the presented method to derive in-plume NO_2 VMRs from MAX-DOAS measurements.

To conclude, the presented measurements provide a real world demonstration that the onion peeling approach works for MAX-DOAS ~~measurments~~ measurements and can successfully be applied to ~~ship emission measurements~~investigate air pollution by ships and to derive in-plume NO_2 volume mixing ratios for ships passing the instrument in a distance of several km.

Data availability. The data used in this study are available from the cited references and directly from the authors upon request.

Competing interests. The authors declare that they have no conflict of interest.

Acknowledgements. The research project which facilitated the reported study was funded in part by the German Federal Maritime and Hydrographic Agency (Bundesamt für Seeschifffahrt und Hydrographie, BSH) and the University of Bremen. The authors thank the Waterways and Shipping Office Cuxhaven (Wasser- und Schifffahrtsamt, WSA), the Hamburg Port Authority (HPA), the AirMAP and NOSE teams and the FU Berlin for their help and support. Many thanks to the editor, Michel Van Roozendael, and to the two anonymous referees for their valuable comments and suggestions, which helped to improve this publication.

References

Alföldy, B., Lööv, J. B., Lagler, F., Mellqvist, J., Berg, N., Beecken, J., Weststrate, H., Duyzer, J., Bencs, L., Horemans, B., Cavalli, F., Putaud, J. P., Janssens-Maenhout, G., Csordás, A. P., Van Grieken, R., Borowiak, A., and Hjorth, J.: Measurements of Air Pollution Emission Factors for Marine Transportation in SECA, Atmospheric Measurement Techniques, 6, 1777–1791, doi:10.5194/amt-6-1777-2013, 2013.

Berg, N., Mellqvist, J., Jalkanen, J. P., and Balzani, J.: Ship Emissions of SO 2 and NO 2: DOAS Measurements from Airborne Platforms, Atmospheric Measurement Techniques, 5, 1085–1098, doi:10.5194/amt-5-1085-2012, 2012.

Gifford, F. A.: Use of Routine Meteorological Observations for Estimating Atmospheric Dispersion, Nuclear Safety, 2, 47–51, 1961.

Gomez, L., Navarro-Comas, M., Puentedura, O., Gonzalez, Y., Cuevas, E., and Gil-Ojeda, M.: Long-Path Averaged Mixing Ratios of O3 and NO2 in the Free Troposphere from Mountain MAX-DOAS, Atmospheric Measurement Techniques, 7, 3373–3386, doi:10.5194/amt-7-3373-2014, 2014.

Hönninger, G., von Friedeburg, C., and Platt, U.: Multi Axis Differential Optical Absorption Spectroscopy (MAX-DOAS), Atmos. Chem. Phys., 4, 231–254, 2004.

IMO: Safety of Life at Sea - Safety of Navigation Chapter V, Tech. rep., International Maritime Organisation (IMO), 2002.

IMO: Resolution MEPC.176(58). Amendments to the Annex of the Protocol of 1997 to Amend the International Convention for the Prevention of Pollution from Ships, 1973, As Modified By the Protocol of 1978 Relating Thereto (Revised MARPOL Annex VI)., Tech. rep., International Maritime Organisation (IMO), 2008.

IMO: Revised MARPOL Annex VI: Regulations for the Prevention of Air Pollution from Ships and NOx Technical Code 2008, International Maritime Organization, London, 2nd edn., 2009.

IMO: Marine Environment Protection Committee (MEPC), 71st Session 3-7 July 2017, http://www.imo.org/en/MediaCentre/MeetingSummaries/MEPC/Pa 71.aspx, 2017.

Lampel, J., Pöhler, D., Tschritter, J., Frieß, U., and Platt, U.: On the Relative Absorption Strengths of Water Vapour in the Blue Wavelength Range, Atmospheric Measurement Techniques, 8, 4329–4346, doi:10.5194/amt-8-4329-2015, 2015.

Martin, D. O.: Comment On"The Change of Concentration Standard Deviations with Distance", Journal of the Air Pollution Control Association, 26, 145–147, doi:10.1080/00022470.1976.10470238, 1976.

Meier, A. C.: Measurements of Horizontal Trace Gas Distributions Using Airborne Imaging Differential Optical Absorption Spectroscopy, Phd thesis, University of Bremen, Bremen, 2018.

Meier, A. C., Schönhardt, A., Bösch, T., Richter, A., Seyler, A., Ruhtz, T., Constantin, D. E., Shaiganfar, R., Wagner, T., Merlaud, A., Van Roozendael, M., Belegante, L., Nicolae, D., Georgescu, L., and Philip Burrows, J.: High-Resolution Airborne Imaging DOAS Measurements of NO2 above Bucharest during AROMAT, Atmospheric Measurement Techniques, 10, 1831–1857, doi:10.5194/amt-10-1831-2017, 2017.

Meller, R. and Moortgat, G. K.: Temperature Dependence of the Absorption Cross Sections of Formaldehyde between 223 and 323 K in the Wavelength Range 225-375 Nm, Journal of Geophysical Research: Atmospheres, 105, 7089–7101, doi:10.1029/1999JD901074, 2000.

Middleton, D. R., Luhana, L., and Sokhi, R. S.: Review of Methods for NO to NO2 Conversion in Plumes at Short Ranges, Environment Agency, Bristol, oCLC: 183145950, 2007.

Ortega, I., Koenig, T., Sinreich, R., Thomson, D., and Volkamer, R.: The CU 2-D-MAX-DOAS Instrument – Part 1: Retrieval of 3-D Distributions of NO2 and Azimuth-Dependent OVOC Ratios, Atmospheric Measurement Techniques, 8, 2371–2395, doi:10.5194/amt-8-2371-2015, 2015.

Pasquill, F.: The Estimation of the Dispersion of Windborne Material., Meteorological Magazin, 90, 33–49, 1961.

Rozanov, V. V., Rozanov, A. V., Kokhanovsky, A. A., and Burrows, J. P.: Radiative Transfer through Terrestrial Atmosphere and Ocean: Software Package SCIATRAN, Journal of Quantitative Spectroscopy and Radiative Transfer, 133, 13–71, doi:10.1016/j.jqsrt.2013.07.004, 2014.

Schönhardt, A., Altube, P., Gerilowski, K., Krautwurst, S., Hartmann, J., Meier, A. C., Richter, A., and Burrows, J. P.: A Wide Field-of-View Imaging DOAS Instrument for Two-Dimensional Trace Gas Mapping from Aircraft, Atmospheric Measurement Techniques, 8, 5113–5131, doi:10.5194/amt-8-5113-2015, 2015.

Schreier, S. F., Richter, A., Wittrock, F., and Burrows, J. P.: Estimates of Free-Tropospheric NO2 and HCHO Mixing Ratios Derived from High-Altitude Mountain MAX-DOAS Observations in the Mid-Latitudes and Tropics, Atmospheric Chemistry and Physics, 16, 2803–2817, doi:10.5194/acp-16-2803-2016, 2016.

Serdyuchenko, A., Gorshelev, V., Weber, M., Chehade, W., and Burrows, J. P.: High Spectral Resolution Ozone Absorption Cross-Sections – Part 2: Temperature Dependence, Atmospheric Measurement Techniques, 7, 625–636, doi:10.5194/amt-7-625-2014, 2014.

Seyler, A., Wittrock, F., Kattner, L., Mathieu-Üffing, B., Peters, E., Richter, A., Schmolke, S., and Burrows, J. P.: Monitoring Shipping Emissions in the German Bight Using MAX-DOAS Measurements, Atmospheric Chemistry and Physics, 17, 10 997–11 023, doi:10.5194/acp-17-10997-2017, 2017.

Sinreich, R., Merten, A., Molina, L., and Volkamer, R.: Parameterizing Radiative Transfer to Convert MAX-DOAS dSCDs into near-Surface Box-Averaged Mixing Ratios, Atmospheric Measurement Techniques, 6, 1521–1532, doi:10.5194/amt-6-1521-2013, 2013.

Thalman, R. and Volkamer, R.: Temperature Dependent Absorption Cross-Sections of O2-O2 Collision Pairs between 340 and 630 Nm and at Atmospherically Relevant Pressure., Physical chemistry chemical physics, 15, 15 371–81, doi:10.1039/c3cp50968k, 2013.

Turner, D. B.: Workbook of Atmospheric Dispersion Estimates, U.S. Dept. of Health, Education, and Welfare, Public Health Service, Environmental Health Service, revised 1970. edn., public Service Publication: no. 999-AP-26. "EPA 742-R-70-001." "Revised 1970.", 1970.

Vandaele, A. C., Hermans, C., Simon, P. C., Roozendael, M. V., Guilmot, J. M., Carleer, M., and Colin, R.: Fourier Transform Measurement of NO2 Absorption Cross-Section in the Visible Range at Room Temperature, J. Atmos. Chem., 25, 289–305, 1996.

Veefkind, J. P., Aben, I., McMullan, K., Förster, H., de Vries, J., Otter, G., Claas, J., Eskes, H. J., de Haan, J. F., Kleipool, Q., van Weele, M., Hasekamp, O., Hoogeveen, R., Landgraf, J., Snel, R., Tol, P., Ingmann, P., Voors, R., Kruizinga, B., Vink, R., Visser, H., and Levelt, P. F.: TROPOMI on the ESA Sentinel-5 Precursor: A GMES Mission for Global Observations of the Atmospheric Composition for Climate, Air Quality and Ozone Layer Applications, Remote Sensing of Environment, 120, 70–83, doi:10.1016/j.rse.2011.09.027, 2012.

Wagner, T., Apituley, A., Beirle, S., Dörner, S., Friess, U., Remmers, J., and Shaiganfar, R.: Cloud Detection and Classification Based on MAX-DOAS Observations, Atmospheric Measurement Techniques, 7, 1289–1320, doi:10.5194/amt-7-1289-2014, 2014.

Wang, Y., Li, A., Xie, P. H., Wagner, T., Chen, H., Liu, W. Q., and Liu, J. G.: A Rapid Method to Derive Horizontal Distributions of Trace Gases and Aerosols near the Surface Using Multi-Axis Differential Optical Absorption Spectroscopy, Atmospheric Measurement Techniques, 7, 1663–1680, doi:10.5194/amt-7-1663-2014, 2014.

Wittrock, F., Oetjen, H., Richter, A., Fietkau, S., Medeke, T., Rozanov, A., and Burrows, J. P.: MAX-DOAS Measurements of Atmospheric Trace Gases in Ny-Ålesund - Radiative Transfer Studies and Their Application, Atmos. Chem. Phys., 4, 955–966, 2004.

Zhang, F., Chen, Y., Tian, C., Lou, D., Li, J., Zhang, G., and Matthias, V.: Emission Factors for Gaseous and Particulate Pollutants from Offshore Diesel Engine Vessels in China, Atmospheric Chemistry and Physics, 16, 6319–6334, doi:10.5194/acp-16-6319-2016, 2016.